Global sensitivities of reactive N and S gas and particle concentrations and deposition to precursor emissions reductions

Yao Ge[1,2,a], Massimo Vieno[2], David S. Stevenson[3], Peter Wind[4], Mathew R. Heal[1]

[1] School of Chemistry, University of Edinburgh, Joseph Black Building, David Brewster Road, Edinburgh, EH9 3FJ, UK
[2] UK Centre for Ecology & Hydrology, Bush Estate, Penicuik, Midlothian, EH26 0QB, UK
[3] School of GeoSciences, University of Edinburgh, Crew Building, Alexander Crum Brown Road, Edinburgh, EH9 3FF, UK
[4] The Norwegian Meteorological Institute, Henrik Mohns Plass 1, 0313, Oslo, Norway
[a] Now at: The Norwegian Meteorological Institute, Henrik Mohns Plass 1, 0313, Oslo, Norway

Correspondence to: Yao Ge (Y.Ge-7@sms.ed.ac.uk), Mathew R. Heal (M.Heal@ed.ac.uk)

Abstract. The reduction of fine particles ($PM_{2.5}$) and reactive N (N_r) and S (S_r) species is a key objective for air pollution control policies because of their major adverse effects on human health, ecosystem diversity, and climate. The sensitivity of global and regional N_r, S_r, and $PM_{2.5}$ to 20% and 40% individual and collective reductions in anthropogenic emissions of NH_3, NO_x, and SO_x (with respect to a 2015 baseline) is investigated using the EMEP MSC-W atmospheric chemistry transport model with WRF meteorology. Regional comparisons reveal that the individual emissions reduction has multiple co-benefits and small disbenefits on different species, and those effects are highly geographically variable. A 40% NH_3 emission reduction decreases regional average NH_3 concentrations by 47-49%, but only decreases NH_4^+ by 18% in Euro_Medi, 15% in East Asia, 12% in North America, and 4% in South Asia. This order follows the regional ammonia-richness. A disbenefit is the increased SO_2 concentrations in these regions (10-16% for 40% reductions) because reduced NH_3 levels decrease SO_2 deposition through altering atmospheric acidity. A 40% NO_x emission reduction reduces NO_x concentrations in East Asia by 45%, Euro_Medi and North America by ~38%, and South Asia by 22%, whilst the regional order is reversed for fine NO_3^-, which is related to enhanced O_3 levels in East Asia (and also, but by less, in Euro_Medi), and decreased O_3 levels in South Asia (and also, but by less, in North America). Consequently, the oxidation of NO_x to NO_3^- and of SO_2 to SO_4^{2-} is enhanced in East Asia but decreased in South Asia, which causes a less effective decrease in NO_3^- and even an increase in SO_4^{2-} in East Asia, but quite the opposite in South Asia. For regional policy making, it is thus vital to reduce three precursors together to minimise such adverse effects. A 40% SO_x emission reduction is slightly more effective in reducing SO_2 (42-45%) than SO_4^{2-} (34-38%), whilst the disbenefit is that it yields ~12% increase in NH_3 total deposition in the four regions which further threatens ecosystem diversity. This work also highlights important messages for policy-makers concerning the mitigation of $PM_{2.5}$. More emissions controls focusing on NH_3 and NO_x are necessary for regions with better air quality such as northern Europe and eastern North America. In East Asia, the three individual reductions are equally effective, whilst in South Asia only SO_x reduction is currently effective. The geographically-varying non-one-to-one proportionality of chemical responses of N_r, S_r, and $PM_{2.5}$ to emissions reductions revealed by this work show the importance of both prioritising emissions strategies in different regions and combining several precursor reductions together to maximise the policy effectiveness.

1 Introduction

Reactive N (N_r) and S (S_r) species are critical determinants of air quality. A substantial proportion of ambient $PM_{2.5}$ (particulate matter with aerodynamic diameter ≤2.5 μm) is secondary inorganic aerosol (SIA) formed from chemical reactions of emissions of the precursor gases NH_3, NO_x (NO and NO_2) and SO_x (sulfur oxides, mainly SO_2) (Behera et al., 2013; Weber et al., 2016; Vasilakos et al., 2018; Nenes et al., 2020). $PM_{2.5}$ is consistently associated with elevated risk of all-cause mortality and other adverse health impacts (Hart et al., 2015; Chen et al., 2017; Chen et al., 2018a; Karimi et al., 2019; Stieb et al., 2020). The gases NO_2 and SO_2 are also direct health pollutants. In addition, oxidized N (e.g., NO_x, HNO_3, and NO_3^-, collectively abbreviated as OXN) and reduced N (e.g., NH_3 and NH_4^+, collectively abbreviated as RDN) species are powerful nutrients for plants and microorganisms, whose deposition leads to eutrophication and loss of ecosystem biodiversity (Erisman et al., 2005; Bergström and Jansson, 2006; Sun et al., 2017; Kharol et al., 2018). The severity of the adverse effects of N deposition is determined not only by the total quantity but also by its form. Many studies show different N deposition components have varying toxicity to different plants, dry deposition of NH_3 is particularly deleterious for example (Van Herk et al., 2003; Sheppard et al., 2011; Sutton et al., 2014, 2020; Pescott et al., 2015) Deposition of oxidized S (i.e., SO_2 and SO_4^{2-}, collectively abbreviated as OXS) also greatly influences precipitation acidity (Lu et al., 2010; Aas et al., 2019; McHale et al., 2021). These observations put greater emphasis on mitigation of certain deposition components.

The East Asia, South Asia, Euro_Medi (Europe and Mediterranean) and North America regions have high population density and high N_r and S_r pollution. Historically, Europe and North America were the dominant emissions regions, suffering severe air pollution until the late 20th century. As reductions in SO_x and NO_x emissions took effect in Europe and North America, emissions in East and South Asia increased dramatically due to rapid industrialisation and dominated global N_r and S_r emissions by the early 21st century (Weber et al., 2016; NEC, 2019; Fowler et al., 2020), although China, in particular, is now implementing effective SO_x and NO_x emissions controls (Liu et al., 2016; Hoesly et al., 2018; Zheng et al., 2018; Meng et al., 2022). In contrast, a lack of action on NH_3 emissions in most countries, coupled with the growth in agriculture to feed a rising global population, means that global NH_3 emissions continue to grow (Heald et al., 2012; Fowler et al., 2015; Aksoyoglu et al., 2020). As a result, ambient N_r and S_r pollution remains a major health and environmental concern in most regions. The European Environmental Agency reported that 97% of the urban population in the European Union in 2019 was exposed to annual mean concentrations of $PM_{2.5}$ above the latest World Health Organization (WHO) air quality guideline of 5 μg m^{-3} (EEA, 2021; WHO, 2021), whilst the United States Environmental Protection Agency reported that for the period 2014-2016 only 10% of its 429 monitoring sites had $PM_{2.5}$ concentrations <6.0 μg m^{-3} (USEPA, 2017). Combining satellite retrievals, chemistry model simulations, and ground level measurements, Ma et al. (2014) and Brauer et al. (2016) showed that in 2013 the majority of the East and South Asia population lived in areas where annual mean $PM_{2.5}$ concentrations exceeded the WHO Interim Target 1 of 35 μg m^{-3} (WHO, 2021). Furthermore, as mitigation of NO_x emissions in recent years has been more effective than for NH_3, deposition of RDN is now increasingly responsible for the exceedances of N critical loads for eutrophication in many regions (Jovan et al., 2012; Chen et al., 2018b; Simpson et al., 2020; Yi et al., 2021; Jonson et al., 2022).

Understanding the sensitivities of $PM_{2.5}$, N_r and S_r pollution to emissions reductions is complicated not only by the substantial regional heterogeneity in relative emissions but also by the substantial meteorological heterogeneity influencing the chemistry and deposition. This necessitates use of atmospheric chemistry transport models (ACTMs) designed to simulate the underlying physical–chemical processes linking emissions, dispersion, chemical reactions, and deposition of atmospheric components. Previous ACTM studies have provided insight into the complexities of sensitivities of $PM_{2.5}$ and its SIA components to changes in emissions in different regions that measurements cannot reveal. For example, using the GEOS-Chem model, Wang et al. (2013) showed that SIA concentrations in 2015 decreased in South China and Sichuan Basin but increased in North China compared to their 2006 levels in response to −16% SO_2 and +16% NO_x emissions changes (no change in NH_3 emissions) from 2006 to 2015 according to China's 12th Five-Year Plan, but if NH_3 emissions increase by +16% (based

on their growth rate from 2006 to 2015), the SIA reduction due to SO_2 reduction will be totally offset in all regions because of the elevated NH_3NO_3 formation, demonstrating the importance of NH_3 control on China's SIA mitigation. Pommier et al. (2018) reported substantial projected growth in emissions in India between 2011 and 2050, amounting to 304% for SO_x, 287% for NMVOC, 162% for NO_x, 100% for primary $PM_{2.5}$, and 60% for CO and NH_3, leading to increases in annual mean $PM_{2.5}$ and O_3 concentrations of 67% and 13% respectively. In the UK, results from EMEP4UK model simulations for 2010 emissions and meteorology indicated that NH_3 emissions reductions are the most effective single-component control (compared to individual reductions in NO_x, SO_x, and primary $PM_{2.5}$) on area-weighted $PM_{2.5}$, whilst weighting by population placed greater emphasis on reductions in emissions of primary $PM_{2.5}$ (Vieno et al., 2016). Holt et al. (2015) used GEOS-Chem to investigate $PM_{2.5}$ sensitivities in the United States to emissions reductions between two sets of scenarios representing a 2005 baseline (high emissions) and a 2012 analogue (low emissions). They found larger sensitivities of $PM_{2.5}$ to SO_x and NO_x controls in the low emissions case since lower NO_x emissions in 2012 enhance the relative importance of aqueous-phase SO_2 oxidation.

These studies analysed N_r and S_r responses to precursor emissions reductions in the early 2000s and in specific regions, but do not provide a global view of sensitivities to the same reductions everywhere. Given the considerable emissions changes in global and regional NH_3, NO_x, and SO_x in recent years (Hoesly et al., 2018; Kurokawa and Ohara, 2020), our understanding of the current chemical climate for N_r and S_r reactions on the global and regional scale and how it affects responses of $PM_{2.5}$, N_r and S_r species to various emissions reductions should be updated. This is the motivation for the work presented here, which provides a global picture of the effectiveness of NH_3, NO_x, and SO_x emissions reductions for mitigating both concentrations and deposition of N_r and S_r pollutants. We used the EMEP MSC-W ACTM to simulate the global domain based on global emissions and meteorology in 2015, which enables a regional comparison to be conducted with inherently consistent simulations. The focus here is on annual means, as these are the long-term metric within global and regional air quality standards. We first describe the model set-up and performance and the sensitivity experiments used to simulate responses of $PM_{2.5}$, N_r and S_r species to 20% and 40% reductions in gaseous precursor emissions (Sect. 2). Section 3 details the global and regional concentration and deposition changes in components of RDN, OXN, OXS, and $PM_{2.5}$ between baseline and emissions reduction scenarios. Section 4 discusses key processes that determine the benefits and disbenefits of emissions reductions and how they vary geographically, and the implications of our findings for policy making.

2 Methods

2.1 Model set-up and performance

The EMEP MSC-W (European Monitoring and Evaluation Programme Meteorological Synthesizing Centre – West) open-source atmospheric chemistry transport model (https://www.emep.int, last access: 8 August 2022) is a three-dimensional Eulerian model widely used for both scientific research and policy development (Bergström et al., 2014; Jonson et al., 2017; Pommier et al., 2018; McFiggans et al., 2019; Karl et al., 2019; Pommier et al., 2020; Jonson et al., 2022). Version rv4.34 was used here. A detailed technical description of EMEP MSC-W rv4.0 is documented in Simpson et al. (2012). A series of overviews of model updates from version rv4.0 to rv4.34 is documented in annual EMEP status reports (Simpson et al., 2013; Tsyro et al., 2014; Simpson et al., 2015, 2016, 2017, 2018, 2019, 2020b). Meteorology for 2015 was derived from the Weather Research and Forecasting model (WRF; https://www.wrf-model.org; https://github.com/wrf-model/WRF/releases/tag/v4.2.2, last access: 8 August 2022) version 4.2.2. The coupled EMEP-WRF system has been tested and applied to many regional and global studies (Vieno et al., 2010, 2014, 2016; Werner et al., 2018; Chang et al., 2020; Gu et al., 2021).

Detailed global EMEP-WRF configurations used in this work are presented in Ge et al. (2021b, 2022). In brief, the global domain has a horizontal resolution of $1° \times 1°$ and 21 terrain-following vertical layers from the surface up to 100 hPa. The height of the lowest model layer is around 45 m. The model outputs of surface concentrations are adjusted to correspond to 3 m above ground level in order to provide concentrations at heights more typical of ambient measurements and human exposure

(Simpson et al., 2012). The aerosol module is the Equilibrium Simplified Aerosol Model V4 (EQSAM4clim), which parameterizes a full gas–liquid–solid partitioning scheme for semi-volatile and non-volatile mixtures. Details are described in Metzger et al. (2016, 2018). Dry deposition of gaseous species and aerosol components to the ground surface is simulated utilizing deposition velocity as described in Simpson et al. (2012, 2020). The parameterisation of wet deposition incorporates both in-cloud and below-cloud scavenging of gases and particles (Berge and Jakobsen, 1998; Simpson et al., 2012).

The global model evaluation of N_r and S_r concentrations and wet deposition from this model configuration for 2010 and 2015 against measurements from 10 ambient monitoring networks is documented in Ge et al. (2021b) and demonstrates the model's capability for capturing the spatial and seasonal variations of NH_3, NH_4^+, NO_2, HNO_3, NO_3^-, SO_2, and SO_4^{2-} in East Asia, Southeast Asia, Europe, and North America. For instance, the correlation coefficients between global model and measurement annual mean concentrations for most species in 2015 are ≥ 0.78, and for annual wet deposition of RDN and OXN are 0.78 and 0.63 respectively. This is in spite of inherent uncertainty in both model and measurements and differences in their spatial representativeness. Section S1 in the Supplement also gives a brief introduction of the model performance compared to measurements for RDN species, as an example.

2.2 Emissions and model experiments

Baseline emissions for 2015 were from the ECLIPSE V6 (Evaluating the CLimate and Air Quality ImPacts of Short-livEd Pollutant) inventory, available at https://previous.iiasa.ac.at/web/home/research/researchPrograms/air/ECLIPSEv6b.html (last access: 8 August 2022). Monthly emissions profiles derived from EDGAR (Emission Database for Global Atmospheric Research, v4.3.2 datasets, available at https://edgar.jrc.ec.europa.eu/dataset_temp_profile) time series (Crippa et al., 2020) were applied to the ECLIPSE annual emissions of SO_2, NO_2, NH_3, CO, CH_4, NMVOC, primary $PM_{2.5}$ and coarse particles. Detailed implementation procedures including the re-assignment of ECLIPSE emissions sectors to EMEP sectors and the calculation of temporal profiles at a given country for a given pollutant are described in Ge et al. (2021b).

A baseline simulation and a set of 8 sensitivity experiments were conducted for emissions and meteorology for 2015. Limited by available computational resources and storage space and taking the achievability of real-world emissions controls into account, the model experiments applied 20% and 40% reductions to global anthropogenic emissions of NH_3, NO_x, SO_x from all sectors both individually and collectively (i.e., reductions applied to all 3 species simultaneously). All other emissions, including natural emissions such as dimethyl sulfide from oceans, lightning NO_x, and soil NO_x, were left unchanged.

The sensitivity ($Sensitivity_i$) of the concentration/deposition of a species *i* is calculated as the absolute difference between the value in baseline ($Baseline_i$) and in an emission reduction scenario ($Scenario_i$). Taking NH_3 concentration as an example:

$$Sensitivity_{NH_3}(\mu g\ m^{-3}) = Baseline_{NH_3} - Scenario_{NH_3}$$

For the relative sensitivity ($Relative\ Sensitivity_i$):

$$Relative\ Sensitivity_{NH_3}(\%) = \frac{Sensitivity_{NH_3}}{Baseline_{NH_3}} \times 100\%$$

The sensitivities of different species are calculated for all emission reduction scenarios. The $PM_{2.5}$ sensitivities derived from individual reductions in emissions of NH_3, NO_x, or SO_x are used to define the sensitivity regimes for different regions in Sect. 3.2. For each model grid, the regime is decided by the precursor that yields the greatest decrease in grid $PM_{2.5}$ concentration: NH_3 sensitive, NO_x sensitive, or SO_x sensitive.

2.3 Definition of world regions

We compared the sensitivities to the emissions reductions of $PM_{2.5}$, N_r and S_r species concentrations and depositions in the four world regions of East Asia, South Asia, Euro_Medi, and North America defined in Fig. 1 (and listed in Table S1). These are based on regions used by the Intergovernmental Panel on Climate Change and as rationalised in Iturbide et al. (2020).

All four regions are densely populated and have high N_r and S_r pollution. Besides, due to limitations in the number of publicly available measurements, our model outputs are evaluated against measurements in East Asia, Europe, and North America, and therefore we have greater confidence in sensitivity results in these three regions. South Asia is chosen because of its extreme ammonia-richness, as revealed by Ge et al. (2022), which makes it an interesting comparison with other regions.

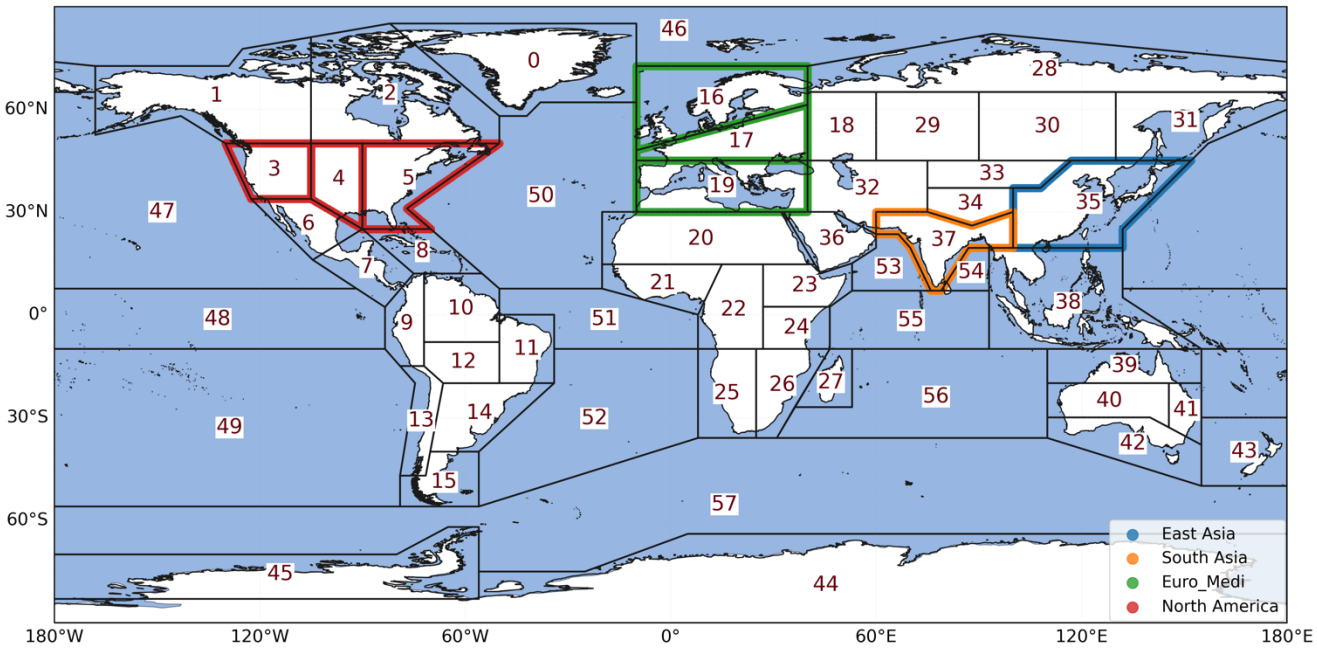

Figure 1: The boundaries of the 4 world regions used in this study, which are based on the IPCC reference regions described in Iturbide et al. (2020).

3 Results

3.1 Sensitivities of N_r and S_r gas and aerosol concentrations

The simulated global baseline 2015 annual mean surface concentrations of N_r and S_r have been discussed in detail in Ge et al. (2022). Here we analyse the sensitivities of the modelled surface concentrations to SIA precursor emissions reductions for RDN, OXN and OXS components. Sensitivities differ according to consideration of primary or secondary components and show great geographical variation.

3.1.1 RDN

Figure 2 shows the spatial variations in the sensitivities of NH_3 and NH_4^+ annual mean surface concentrations to 20% and 40% emissions reductions in NH_3, NO_x, and SO_x individually, and collectively. Regional average sensitivities in East Asia, South Asia, Euro_Medi, and North America are summarised in Fig. 3 and Table S2. Steeper gradients in Fig. 3 correspond to greater concentration changes (sensitivities).

From these figures, it is clear that whilst reducing emissions of NH_3 (and all 3 precursors together) decrease NH_3 concentrations efficiently, reducing emissions of NO_x or SO_x lead to increases in NH_3 concentrations, particularly over densely populated areas. The maximum reduction in model grid NH_3 concentration across all scenarios reaches 16.6 μg m^{-3} (44% change relative to baseline; expressed similarly hereafter) and occurs over East Asia in response to a 40% reduction in NH_3 emissions. The largest increase in NH_3 concentration (1.51 μg m^{-3}, 22%) arises in Southeast Asia under the 40% SO_x emissions reduction scenario. Lower NO_x and SO_x emissions decrease the concentration of acidic species available to react with NH_3 to form NH_4^+ aerosol, so more of the emitted NH_3 stays in the gas phase. Other studies have likewise shown that reductions in

SO_2 or NO_x emissions are an important contributor to the growth in tropospheric NH_3 concentrations globally and regionally (Saylor et al., 2015; Warner et al., 2017; Liu et al., 2018; Yu et al., 2018).

In East Asia and North America, NH_3 concentrations increase similarly for either NO_x or SO_x reductions (Fig. 3), but in South Asia and Euro_Medi, NH_3 concentrations increase more with SO_x reductions than with NO_x reductions, which reflects the larger contribution of $(NH_4)_2SO_4$ than NH_4NO_3 to SIA in the latter two regions. However, the increase in NH_3 concentrations is relatively small compared to the extent of NO_x and SO_x emissions reductions: 40% reductions in emissions of NO_x or SO_x only increase NH_3 concentrations in the 4 regions by 2-6% or 6-9%, respectively (Fig. 3, Table S2). The globally averaged increases in NH_3 concentrations for 40% reductions in NO_x or SO_x emissions are 3% and 9%, respectively. Nevertheless, the NH_3 concentration decrease resulting from reductions in NH_3 emissions is offset by simultaneous effects of NO_x and SO_x emissions reductions when all 3 precursors are reduced together, as the sensitivities of regional average NH_3 concentrations to 40% reductions in all 3 precursor emissions (38-39% across the four regions) are smaller than their sensitivities to 40% reductions in NH_3 emissions on its own (47-49%). It is also noteworthy that the sensitivities of regional average NH_3 concentrations are essentially linear through 20% and 40% emissions reductions, irrespective of precursor, although the sensitivities are different between regions.

In contrast to NH_3, concentrations of NH_4^+ always decrease when an SIA precursor emission is reduced. Figure 2 shows that NH_4^+ concentrations in the most densely populated continents (e.g., eastern China, India, Europe, eastern America) respond strongly to emissions reductions in each SIA precursor, whilst they only respond to SO_x emissions reductions over oceans. This is related to the production of marine sulfate aerosol from dimethyl sulfide (DMS) and the lack of significant oceanic NO_x emissions sources, which means only $(NH_4)_2SO_4$ formation is important in marine SIA chemistry.

In addition, the impacts of NH_3 and SO_x emissions reductions on NH_4^+ concentrations over North Africa are significantly greater than from NO_x emissions reductions, indicating a dominance of $(NH_4)_2SO_4$ within SIA in this region. This is consistent with the results reported by Ge et al. (2022). They showed that large areas in North Africa are characterised by the SO_4^{2-}-rich chemical domain for SIA formation, which means that NH_3 is predominantly taken up by SO_4^{2-}, leaving no free NH_3 to react with HNO_3 to form NH_4NO_3. Given that emissions reductions in all three precursors individually lead to reductions in NH_4^+ concentrations, it is not surprising that the greatest simulated NH_4^+ reduction (5.87 μg m^{-3} (43%) in East Asia) arises for the scenario with 40% reductions in all 3 precursors collectively.

Figure 3 also shows that NH_4^+ sensitivities are essentially linear for emissions reductions to 40%, although responses again vary slightly with region. Among individual precursor reduction scenarios, regional average NH_4^+ concentrations in East Asia and Euro_Medi are most sensitive to SO_x emissions reductions and least sensitive to NO_x reductions, while NH_4^+ concentrations in North America are most sensitive to SO_x reductions and least sensitive to NH_3 reductions. In South Asia, NH_4^+ is characterised by strong sensitivity to SO_x emissions reductions but only relatively small sensitivities to NO_x and NH_3 emissions reductions. In the scenario of all 3 species reductions, all regions show relative sensitivities close to the one-to-one line. Another important observation from Fig. 3 is that reductions in NH_4^+ (4-18%) in response to a 40% NH_3 emissions reduction are much smaller than reductions of NH_3 concentrations (47-49%) in these regions, which reflects the fact that these regions are so ammonia-rich that reducing NH_3 emissions only has limited effects on NH_4^+ concentrations.

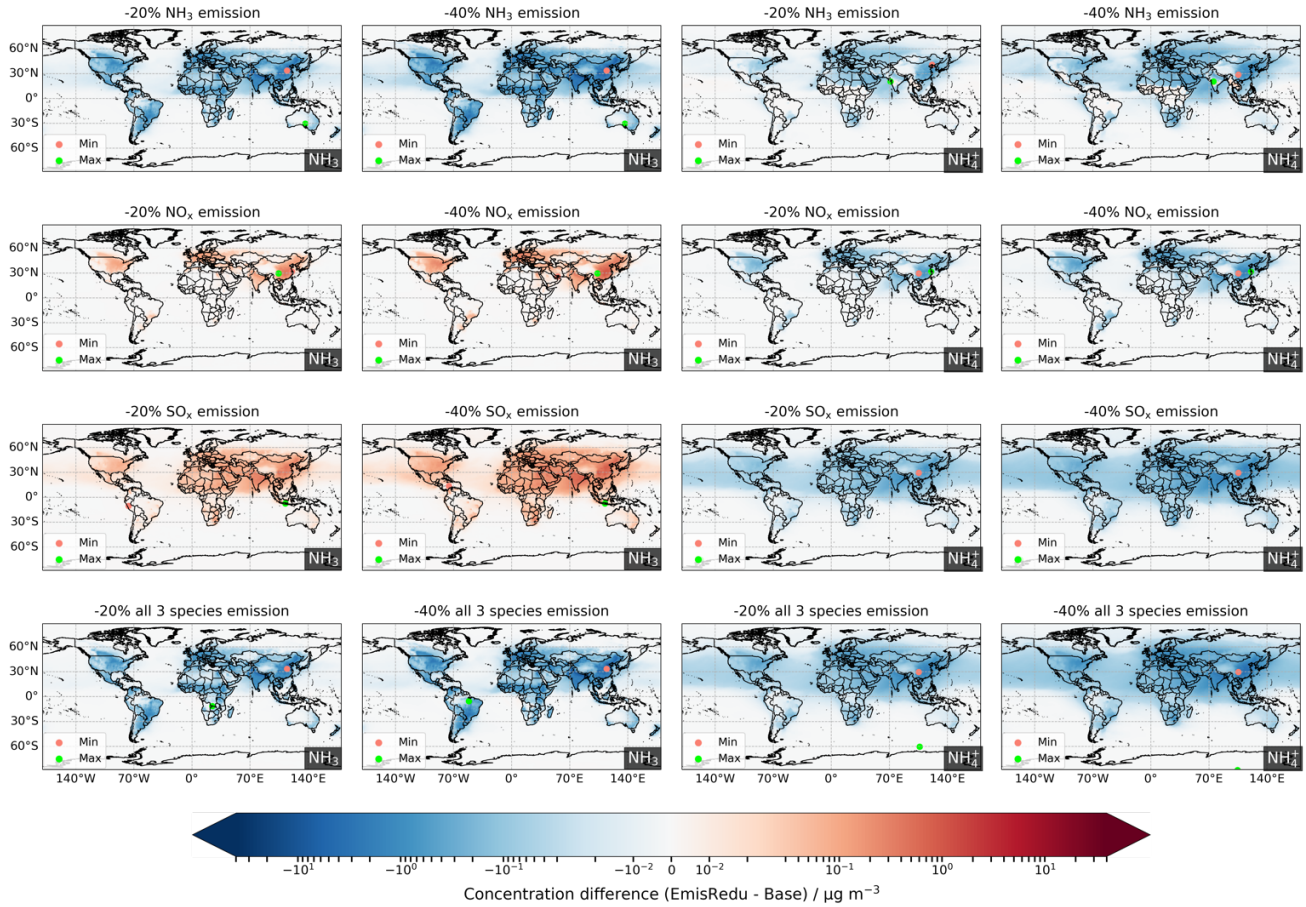

Figure 2: Changes in NH_3 and NH_4^+ annual surface concentrations for 20% and 40% emissions reductions in NH_3, NO_x, and SO_x individually and collectively. Red and green dots in each map locate the minimum and maximum difference, respectively.

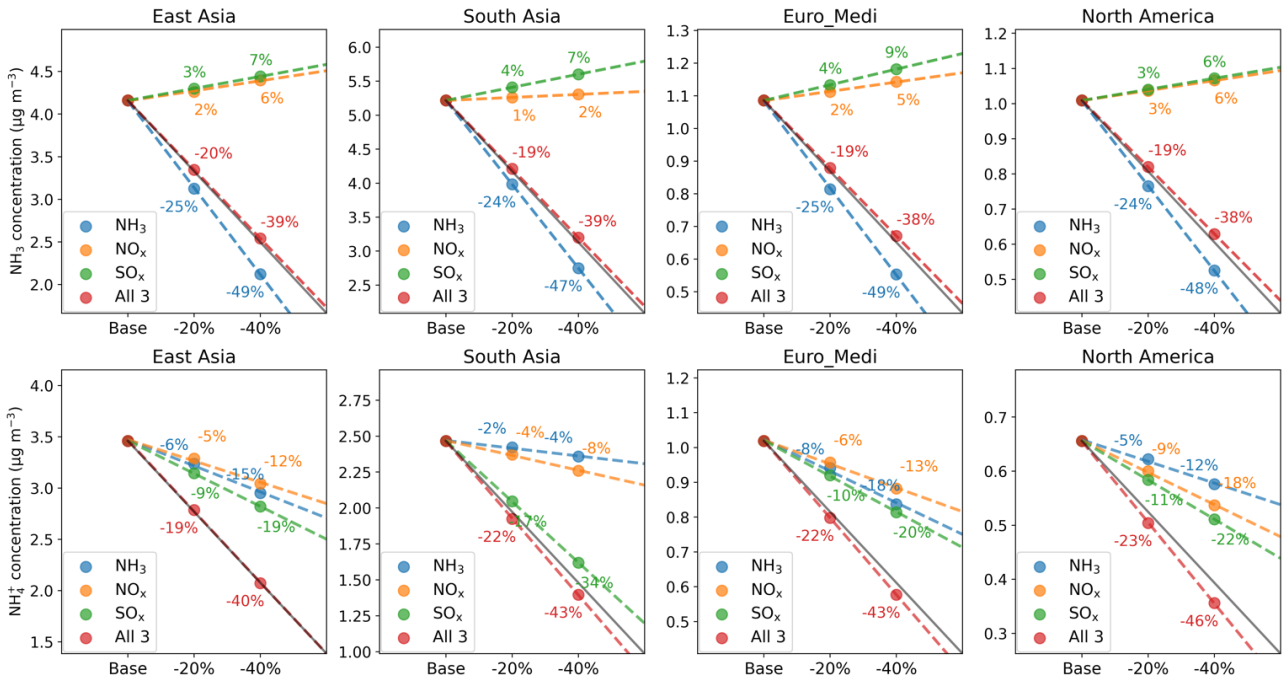

Figure 3: The absolute and relative sensitivities of regionally-averaged annual mean surface concentrations of NH_3 (upper row) and NH_4^+ (lower row) to 20% and 40% emissions reductions in NH_3 (blue), NO_x (orange) and SO_x (green) individually, and collectively (red), for the four regions defined in Fig. 1. The solid grey line in each panel illustrates the one-to-one relative response to emissions reductions, whilst the coloured dashed lines are the linear regressions through each set of three model simulations and illustrate the actual responses to emissions reductions of a given precursor. The numbers show the corresponding relative responses to each emissions reduction (with respect to baseline).

3.1.2 OXN

Figure 4 shows the spatial variations in the sensitivities of NO_x and fine nitrate annual mean surface concentrations to 20% and 40% emissions reductions in NH_3, NO_x, and SO_x individually, and collectively. Regional average sensitivities in East Asia, South Asia, Euro_Medi, and North America are summarised in Fig. 5 and Table S3. Equivalent global maps and regional sensitivity plots for the responses of HNO_3 and coarse nitrate to the same emissions reductions are presented in Figs. S2 and S3 and Table S3.

In contrast to surface NH_3, whose concentrations are sensitive to reductions in emissions of each of NH_3, NO_x and SO_x, surface NO_x concentrations only respond to NO_x emissions reductions and have negligible sensitivity to NH_3 and SO_x emissions reductions. The 20% and 40% reductions in NO_x emissions yield a global maximum of 25.6 $\mu g\ m^{-3}$ (22%) and 51.3 $\mu g\ m^{-3}$ (44%) reductions in surface NO_x concentrations over East Asia. The globally averaged reductions in NO_x concentrations for 20% and 40% reductions in NO_x emissions are 15% and 30% respectively (same values for simultaneous reductions in all 3 precursors), whereas the sensitivities for NH_3 and SO_x emissions reduction are all 0% (Table S3).

Regionally (Fig. 5), East Asia shows the largest decreases in NO_x concentrations (45%) in response to 40% NO_x emissions reductions, followed by Euro_Medi and North America (36-38%), and South Asia (23%). These regional differences in sensitivities to NO_x emissions are due to regional differences in oxidation chemistry climate. Figure S4 shows the changes in annual mean surface concentrations of O_3 for the 8 emissions reduction scenarios. Concentrations of O_3 in eastern China, western and central Europe, and north-eastern US increase as NO_x emissions reduce, while O_3 in the rest of the world decreases as NO_x emissions reduce. In East Asia, the increased oxidant levels enhance NO_x chemical removal and results in a greater than one-to-one relative decrease in NO_x concentrations with NO_x emissions reductions. Consequently, the decrease in fine nitrate in East Asia is offset by enhanced chemical production, which leads to a lower than one-to-one sensitivity (e.g., a 40% reduction in NO_x emissions gives a 33% decrease in fine NO_3^-). In contrast, decreased oxidant levels in South Asia decrease the oxidation of NO_x, which partially offsets the decrease in NO_x concentrations induced by emissions reductions, causing a more efficient reduction in fine NO_3^- concentrations than in NO_x in this region. The variation in regional atmospheric oxidising capacity also alters the SO_4^{2-} formation processes; discussions of this are presented in Sect.3.1.3 and Sect. 4. The situation is more complex for Euro_Medi and North America as these regions include both positive and negative changes in O_3 concentrations with NO_x emissions reductions (Fig. S4) and they are not as NO_x-rich as East Asia and South Asia. The effects of changes in oxidant levels on NO_x and fine NO_3^- concentrations are therefore more localised and less apparent in regional averages. Clappier et al. (2021) reported this effect to be most distinct in the Po basin (Italy), western Germany, and Netherlands in Europe, whilst for the United States, Tsimpidi et al. (2008) showed it only becomes pronounced in the northeast, both of which are consistent with our results.

For secondary OXN species, the sensitivities of HNO_3 and fine and coarse NO_3^- to individual reductions in emissions of NH_3, NO_x and SO_x are closely associated with SIA formation chemistry. The principal observation from Fig. 4 is that concentrations of fine NO_3^- in all four regions decrease with reduced NH_3 and NO_x emissions but increase with reduced SO_x emissions. This is because H_2SO_4 and HNO_3 compete in their reactions with NH_3, and $(NH_4)_2SO_4$ is formed preferably over NH_4NO_3. Reductions in NH_3 emissions cause the equilibrium between HNO_3 and NH_3 to shift away from NH_4NO_3 production and therefore free more HNO_3 molecules. As a result, more HNO_3 is available to produce coarse nitrate aerosol, leading to a decrease in fine NO_3^- but an increase in coarse NO_3^- concentrations (Fig. S2). Reductions in NO_x emissions decrease HNO_3 and fine and coarse NO_3^- concentrations globally. Although the increased oxidant levels that arise in some regions following NO_x emissions reductions enhance the chemical formation of these secondary species (as discussed above), NO_x emissions reductions of 20% and 40% are substantial enough to mean that the lower availability of NO_x to form NO_3^- dominates the impact on NO_3^- concentrations compared with the enhancement in oxidising capacity. Reduced SO_x emissions leave more NH_3 to equilibrate with HNO_3 to form NH_4NO_3, leading to an increase in fine NO_3^- concentrations but to a decrease in coarse NO_3^- concentrations as the former takes more HNO_3. It is notable that the increase in fine NO_3^- concentrations is relatively small

compared to the extent of SO_x emissions reductions. For example, the maximum increase in fine NO_3^- resulting from 40% reductions in SO_x emissions is 1.71 μg m^{-3} (16%), in East Asia. The regional average increases in fine NO_3^- concentrations for 40% SO_x emissions reductions are 8% in East Asia, South Asia, and Euro_Medi, and 4% in North America.

The differences in regional average sensitivities of HNO_3 and fine and coarse NO_3^- are highlighted more clearly in Fig. 5 and Fig. S2. Fine NO_3^- in East Asia is equally sensitive to NO_x and NH_3 emissions reductions (33% and 32% decreases for 40% NO_x and NH_3 emissions reductions respectively), while it is more sensitive to NO_x emissions reductions than to NH_3 emissions reductions in South Asia (45% and 39%), Euro_Medi (41% and 33%), and North America (42% and 26%). In terms of absolute concentration changes, the reductions in fine NO_3^- over East Asia in response to 40% NH_3 and NO_x emissions reductions (1.62 -1.65 μg m^{-3}) are more than 3 times larger than reductions in other regions (0.23 - 0.47 μg m^{-3}). On the other hand, if NH_3 emissions are reduced then the increases in HNO_3 and coarse NO_3^- concentrations in East Asia (15% increases for 40% NH_3 reductions) are much larger than the increases in the other three regions (2-6%). All these differences between East Asia and the other three regions reflect the larger abundance of NH_4NO_3 in SIA over East Asia. This is demonstrated in Fig. S8 which shows that the contribution of fine NO_3^- to $PM_{2.5}$ in the baseline is greatest in East Asia (19%, 5.21 μg m^{-3}), followed by Euro_Medi (12%, 1.22 μg m^{-3}), North America (11%, 0.86 μg m^{-3}), and South Asia (3%, 0.93 μg m^{-3}). Detailed discussion on regional SIA composition is presented in Sect. 3.2.

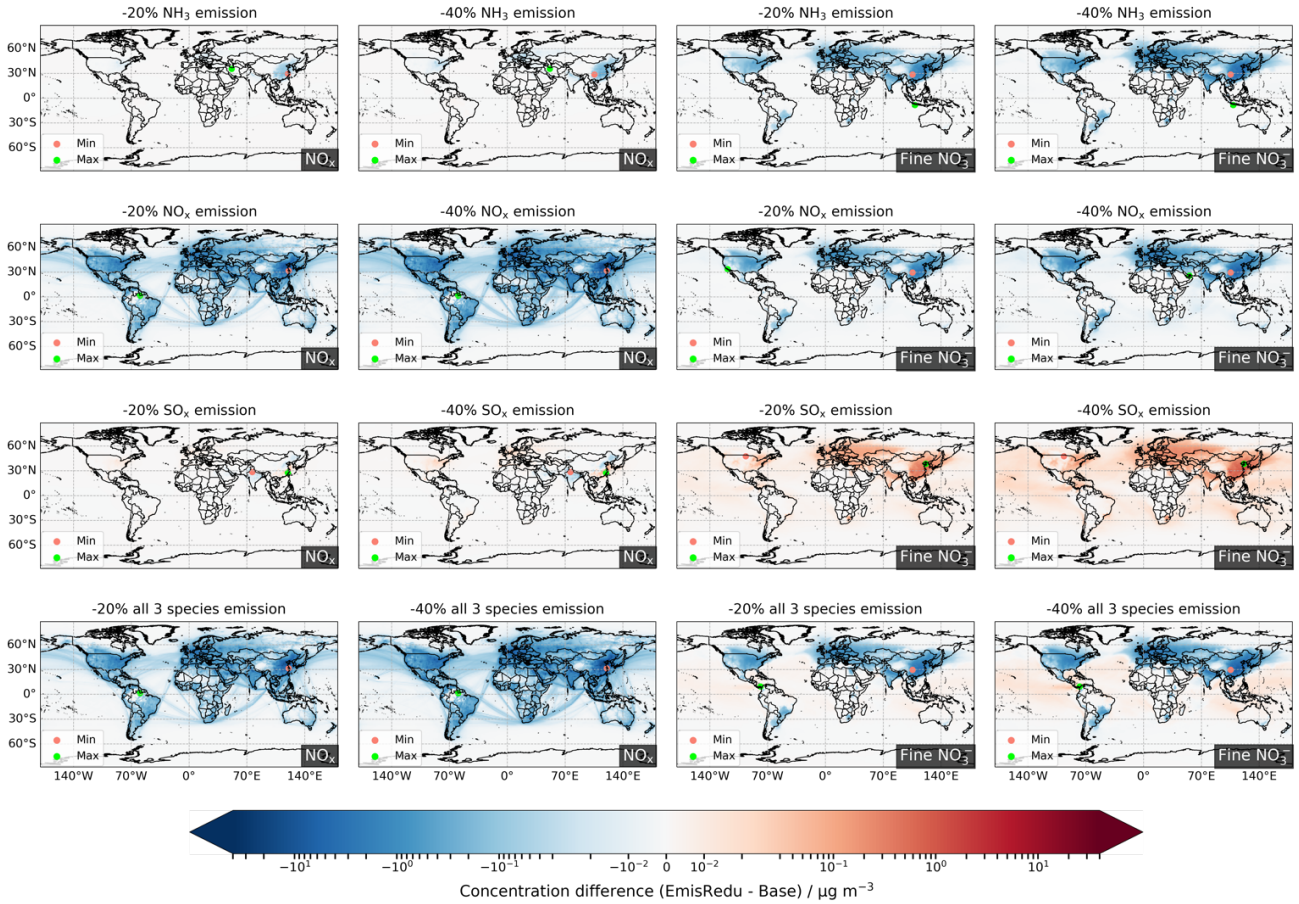

Figure 4: Changes in NO_x and fine NO_3^- annual surface concentrations for 20% and 40% emissions reductions in NH_3, NO_x, and SO_x individually and collectively. Red and green dots in each map locate the minimum and maximum difference, respectively.

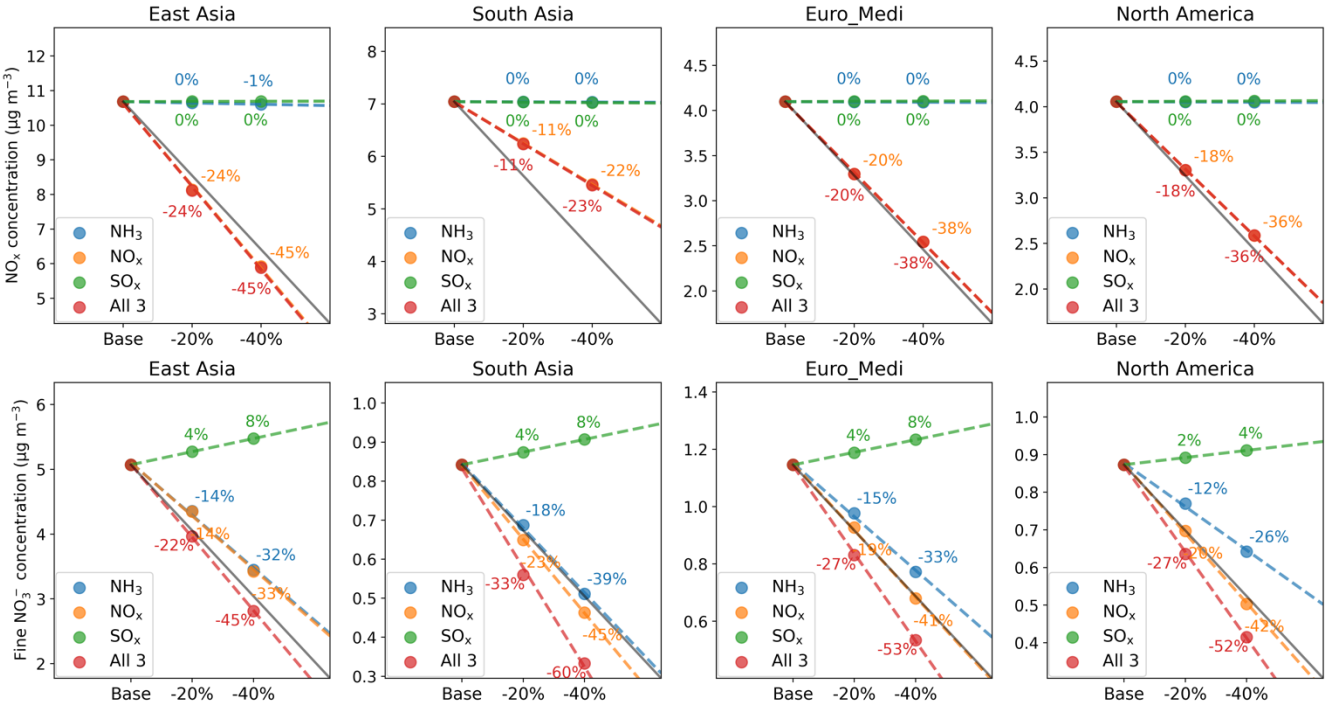

Figure 5: The absolute and relative sensitivities of regionally-averaged annual mean surface concentrations of NOx (upper row) and fine NO_3^- (lower row) to 20% and 40% emissions reductions in NH_3 (blue), NO_x (orange) and SO_x (green) individually, and collectively (red), for the four regions defined in Fig. 1. The solid grey line in each panel illustrates the one-to-one relative response to emissions reductions, whilst the coloured dashed lines are the linear regressions through each set of three model simulations and illustrate the actual responses to emissions reductions of a given precursor. The numbers show the corresponding relative responses to each emissions reduction (with respect to baseline).

3.1.3 OXS

Figure 6 shows the global variation in the sensitivities of SO_2 and SO_4^{2-} annual mean surface concentrations to 20% and 40% emissions reductions in NH_3, NO_x, and SO_x individually, and collectively. Figure 7 and Table S4 summarise the sensitivities of the regionally averaged SO_2 and SO_4^{2-} concentrations to the emissions reductions for the four regional domains. Concentrations of SO_2 increase in response to reduced NH_3 emissions particularly over East Asia, South Asia, Europe, and North America. The largest increases in SO_2 resulting from 20% and 40% NH_3 emissions reductions are respectively in Southeast Asia (3.62 μg m^{-3}, 9%) and East Asia (8.11 μg m^{-3}, 20%) (Fig. 6). The response of secondary SO_4^{2-} concentrations to NH_3 emissions reductions varies substantially across the world. In north-eastern China and Europe, SO_4^{2-} concentrations increase, whilst in southern China, India, and United States they decrease. However, the magnitudes of SO_4^{2-} concentration changes are much smaller than for SO_2. The maximum increases in SO_4^{2-} concentrations (located in southern China) are only 0.37 μg m^{-3} (2%) and 0.89 μg m^{-3} (5%) for 20% and 40% NH_3 emissions reductions, respectively. The maximum decreases in SO_4^{2-} concentrations, in north-eastern China, are 0.62 μg m^{-3} (6%) and 1.30 μg m^{-3} (12%), respectively. Regionally averaged, East Asia exhibits the largest increase in SO_2 for 40% NH_3 emissions reductions (16%) (Fig. 7) followed by North America (14%), South Asia (14%), and Euro_Medi (10%), whereas increases in regional average SO_4^{2-} concentrations are only in the range 0-2%.

Figures S5 and 13 show the global variation in the sensitivities to precursor emissions reductions of total deposition of SO_2, and of the wet and dry deposition of all OXS components, respectively. When NH_3 emissions are reduced, SO_2 total deposition decreases over all of East Asia, South Asia, Europe, and North America (Fig. S5); Fig. 13 shows the decrease is driven by reduced SO_2 dry deposition. Several studies have shown that the non-stomatal canopy uptake resistance of SO_2 (the inverse of the SO_2 dry deposition velocity) is positively correlated to the molar 'acidity ratio' $a_{SN} = \frac{[SO_2]}{[NH_3]}$ (Smith et al., 2000; Erisman et al., 2001; Fowler et al., 2009; Massad et al., 2010), a process that is included in the EMEP MSC-W model (Simpson

et al., 2012). Reduced NH_3 concentrations therefore increase the acidity ratio and hence decrease the rate of SO_2 dry deposition and increase the SO_2 surface concentrations in those regions where this effect is significant. The SO_4^{2-} responses to NH_3 emissions reductions are related to changes in atmospheric acidity as well. The aqueous-phase oxidation of SO_2 by O_3, which is one of the major pathways for SO_4^{2-} production, is significantly pH dependent. In general, the oxidation rate decreases with decreased pH (Penkett et al., 1979; Maahs, 1983; Liang and Jacobson, 1999; Hattori et al., 2021), a process that is incorporated into the EMEP MSC-W model (Simpson et al., 2012). As pointed out by Ge et al. (2022), Europe and north-eastern China are much less ammonia-rich than India, which means that 20% and 40% NH_3 emissions reductions are substantial enough to decrease the pH in the former two regions, leading to decreases in SO_4^{2-} production. However, given that SO_2 levels increase and that there are still other effective oxidation pathways (e.g., OH, H_2O_2) which are independent of pH (McArdle and Hoffmann, 1983; Hoffmann, 1986; Seinfeld and Pandis, 2016), the decreases in SO_4^{2-} concentrations in Europe and north-eastern China due to NH_3 emissions reductions are very small anyway. In contrast, since India is so ammonia-rich, even 40% reductions in NH_3 emissions do not significantly alter the pH in this region. As a result, SO_4^{2-} concentrations in India increase slightly due to the higher availability of its precursor SO_2.

The impacts of NO_x emissions reductions on SO_2 concentrations show inverse trends in different regions (Fig 7), which reflects regional differences in atmospheric oxidation chemistry. The decreased SO_2 concentrations (maximum reduction: 1.72 μg m^{-3}, 6%) in eastern China, Europe, and north-eastern United States (Fig. 6) can be explained by the enhanced O_3 concentrations in these regions arising from the reduced NO + O_3 reaction in these high NO_x regions (Fig. S4). As a result, SO_2 is more readily oxidised to SO_4^{2-}, leading to increased SO_4^{2-} concentrations (maximum increase for 40% NO_x emissions reductions: 1.59 μg m^{-3} (10%)) in these regions. This positive response of SO_4^{2-} to NO_x emissions reductions is also reported in regional studies (Botha et al., 1994; Li et al., 2006; Sheng et al., 2018; Fang et al., 2019; Ge et al., 2021a). In contrast, India, north-eastern Africa, and southern Africa show increased SO_2 (maximum increase: 0.29 μg m^{-3}, 1%) but decreased SO_4^{2-} concentrations (maximum decrease: 0.73 μg m^{-3}, 9%) as NO_x emissions reduce, which can be explained by the parallel decrease in O_3 concentrations in these regions (Fig. S4). However, these concentration changes are very localised and, from a regional average perspective, are relatively small compared to the extent of emissions reductions applied. For example, in East Asia, the region with the largest response, there is only a 5% decrease in regional average SO_2 concentration (Fig. 7), and 3% increase in SO_4^{2-} concentration, for a 40% reduction in NO_x emissions. For other regions, the SO_2 and SO_4^{2-} regional average concentration changes are even smaller (from -4% to 2%). The global average sensitivities of SO_2 and SO_4^{2-} annual mean concentrations to 20% and 40% NO_x emissions reductions are only in the range 0-2% (Table S4).

Under reductions of SO_x emissions (and of all 3 precursors together), both SO_2 and SO_4^{2-} show almost one-to-one reductions, indicating that SO_x emissions reductions are crucial for reducing both primary and secondary OXS pollutants and, in the case of reductions of all 3 precursors simultaneously, readily sufficient to dominate over any tendency for NH_3 and NO_x emissions reductions to increase OXS species concentrations. A 40% reduction in SO_x emissions leads to a maximum SO_2 decrease of 39.8 μg m^{-3} (40%), in northern Russia, and a maximum SO_4^{2-} decrease of 7.70 μg m^{-3} (39%), in south-eastern China (Fig. 6). For the four regions, average SO_2 concentrations decrease by 22-24% and 42-45%, and SO_4^{2-} concentrations decrease by 17-19% and 34-38%, in response to 20% and 40% SO_x emissions reductions respectively (Fig. 7). For the 20% and 40% reductions in all 3 precursors together, regionally averaged SO_2 decrease by 19-20% and 38-41% respectively, and regionally averaged SO_4^{2-} decrease by 17-20% and 35-40% respectively.

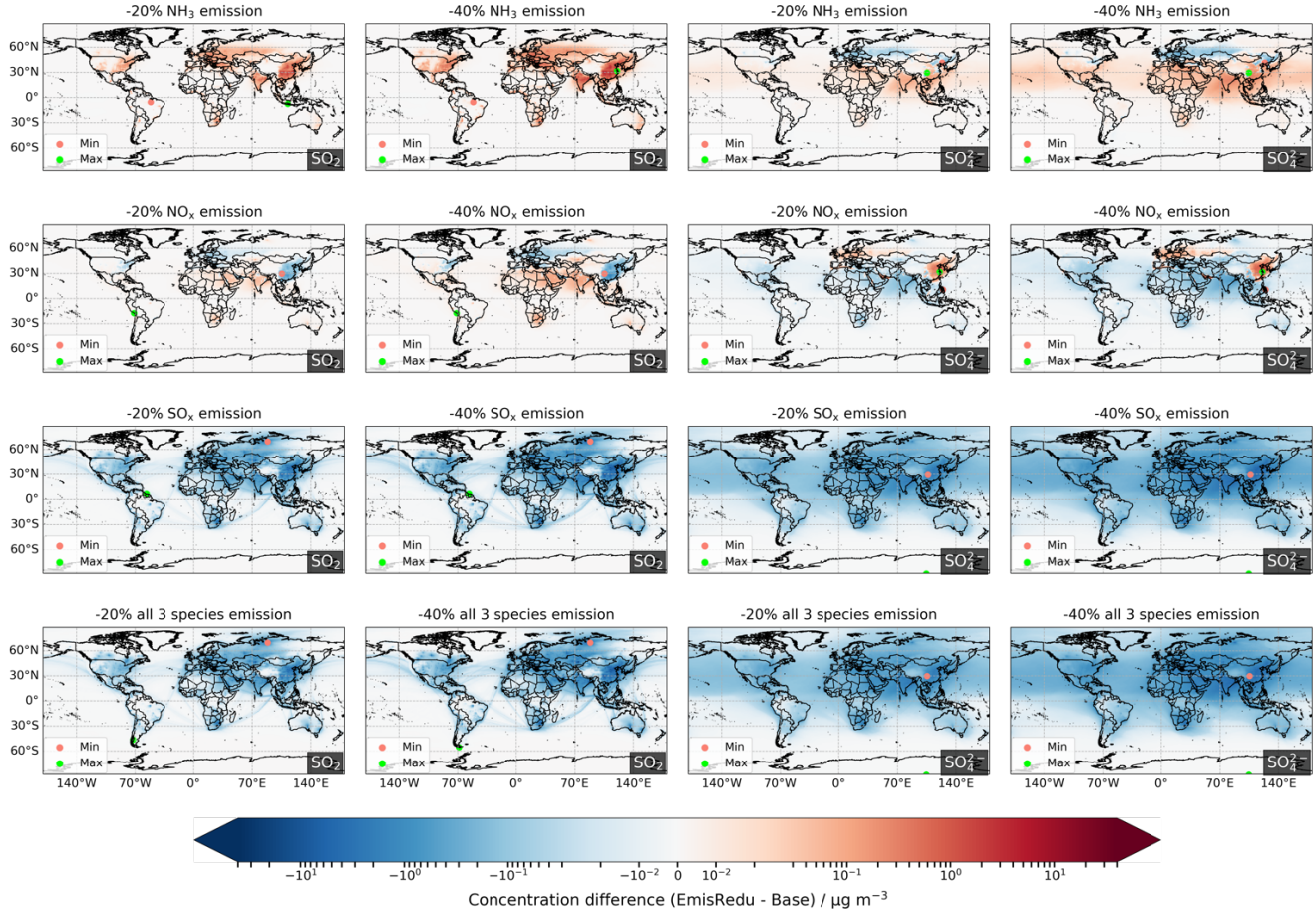

Figure 6: Changes in SO_2 and SO_4^{2-} annual surface concentrations for 20% and 40% emissions reductions in NH_3, NO_x, and SO_x individually and collectively. Red and green dots in each map locate the minimum and maximum difference, respectively.

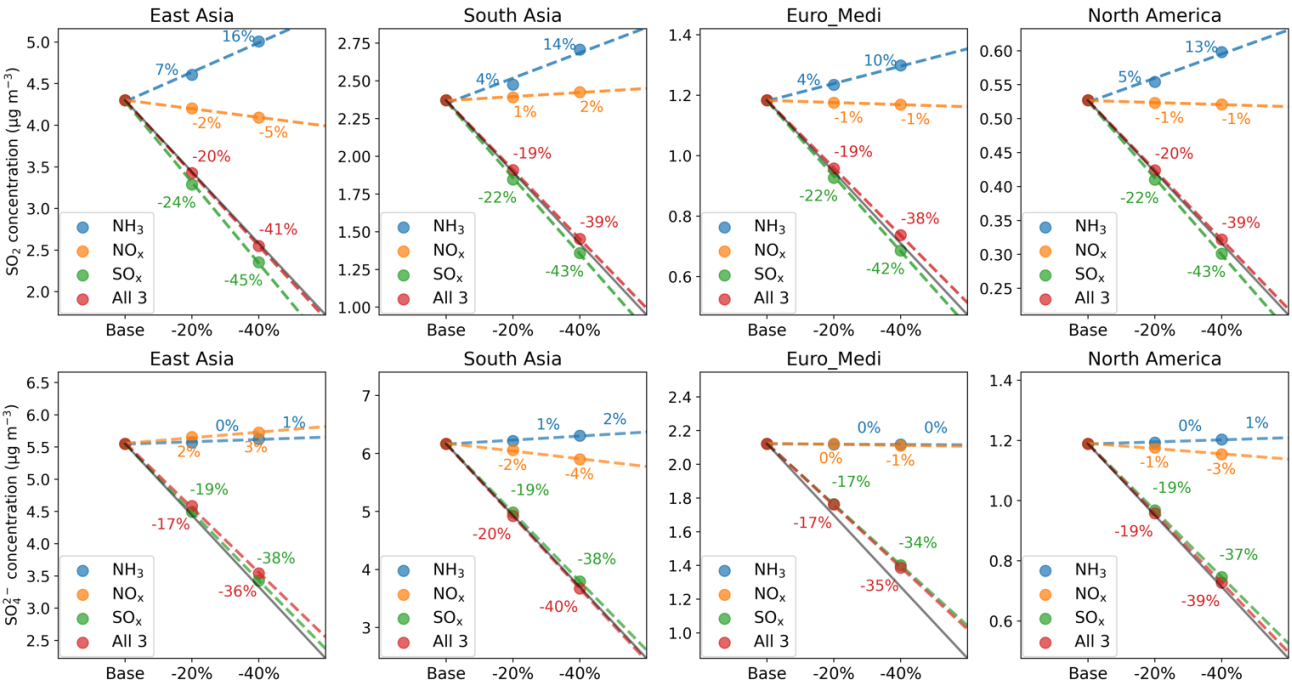

Figure 7: The absolute and relative sensitivities of regionally-averaged annual mean surface concentrations of SO_2 (upper row) and SO_4^{2-} (lower row) to 20% and 40% emissions reductions in NH_3 (blue), NO_x (orange) and SO_x (green) individually, and collectively (red), for the four regions defined in Fig. 1. The solid grey line in each panel illustrates the one-to-one relative response to emissions reductions, whilst the coloured dashed lines are the linear regressions through each set of three model simulations and illustrate the actual responses to emissions reductions of a given precursor. The numbers show the corresponding relative responses to each emissions reduction (with respect to baseline).

3.2 Sensitivity of $PM_{2.5}$ concentrations

Figure 8 shows the global distribution of the dominant sensitivity of $PM_{2.5}$ towards a 40% reduction in NH_3, NO_x, or SO_x emissions individually. An annual mean $PM_{2.5}$ concentration threshold of 5 μg m^{-3} has been applied in order to focus attention on more polluted areas where $PM_{2.5}$ concentrations in the baseline simulation are above the latest WHO $PM_{2.5}$ air quality guideline (AQG) (WHO, 2021). Section S2 and Fig. S7 in the Supplement present seasonal variations in global $PM_{2.5}$ sensitivity regimes.

The principal observation from Fig. 8 is that the sensitivity of $PM_{2.5}$ to reductions in emissions of individual precursors is highly geographically variable. SO_x-sensitive regimes are found in Southeast Asia, South Asia, Africa, and Central America. NO_x-sensitive regimes are observed in south-eastern China, France, Germany, most eastern European countries, central and eastern United States, and northern and central parts of South America. Only a few small regions are NH_3 sensitive: these include eastern coastal areas around China, the UK and its surrounding seas, southern Scandinavia, and western Russia. The difference in $PM_{2.5}$ sensitivity between northern Europe and the rest of Europe demonstrates that NH_3 has become the limiting factor for SIA formation in northern Europe. This greater leverage of NH_3 emissions on $PM_{2.5}$ mitigation in this region is due to the effective emissions controls on all SIA precursor emissions here (see also Sect. 4 discussion) (Tørseth et al., 2012; AQEG, 2015; Vieno et al., 2016; Ciarelli et al., 2019; Theobald et al., 2019). In contrast, South Asia is so ammonia-rich that reducing NH_3 concentrations has little impact on $PM_{2.5}$ (Ge et al., 2022). The situation in northern Europe exemplifies what to expect in terms of future policy making for the rest of the world. Furthermore, many marine areas are characterised as SO_x sensitive but for a different reason than the SO_x-sensitive regime in South Asia. In the marine areas, fine nitrate and ammonium aerosols are relatively small compared to sulfate aerosols, therefore reductions in NO_x and NH_3 emissions hardly affect SIA formation. In fact, sulfate aerosol derived from oceanic emissions of DMS rather than from anthropogenic emissions is the major contributor to marine $PM_{2.5}$ (Quinn and Bates, 2011; Hoffmann et al., 2016; Novak et al., 2022).

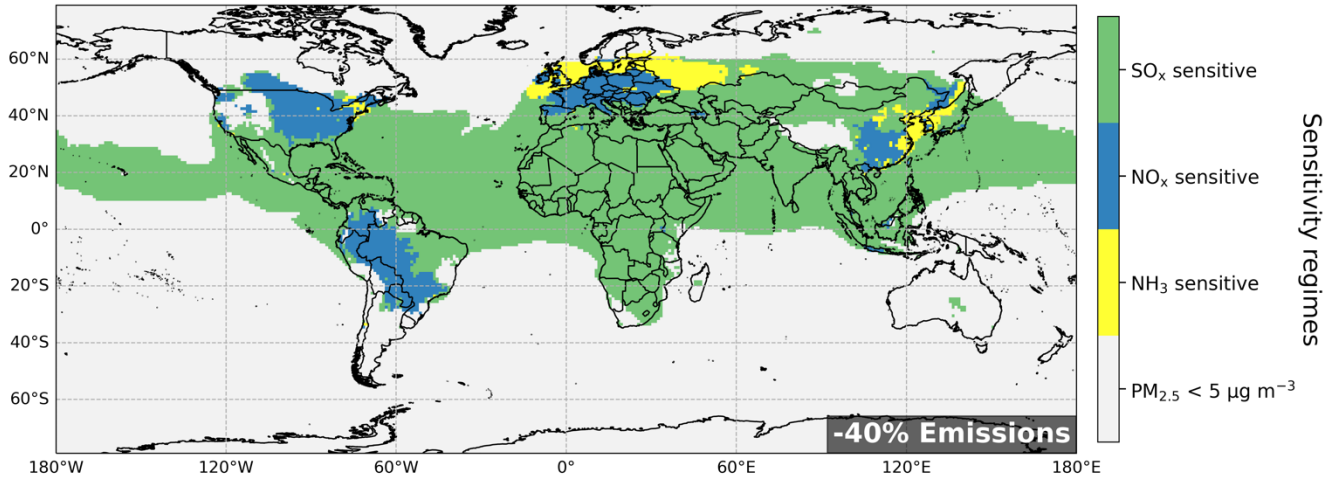

Figure 8: Spatial variation in sensitivity regime of $PM_{2.5}$ mitigation based on data from 40% individual reductions in emissions of NH_3, NO_x, or SO_x. The regime is defined according to the precursor that yields the greatest decreases in grid $PM_{2.5}$ concentration: NH_3 sensitive (yellow), NO_x sensitive (blue), SO_x sensitive (green). Model grids with baseline annual mean $PM_{2.5}$ concentrations <5 μg m^{-3} are masked out.

Detailed examination of the magnitudes of the $PM_{2.5}$ sensitivities in each location to each precursor (rather than just their ranking) reveals more complicated regional characteristics. Figure 9 shows the spatial variabilities in $PM_{2.5}$ sensitivities to 40% reductions in emissions of NH_3, NO_x, and SO_x individually, and collectively, for the four world regions. The regionally averaged $PM_{2.5}$ sensitivities are summarised in Fig. 10 and Table S5. $PM_{2.5}$ concentrations in East Asia show comparable sensitivities to individual emissions reductions in NH_3, NO_x, and SO_x, with the impacts of NH_3 and NO_x emissions reductions

being more concentrated in continental areas than those for SO_x emissions reductions (Fig. 9). A 40% reduction in NO_x emissions yields a maximum decrease in $PM_{2.5}$ of 11.5 μg m^{-3} (12%) over southern China, while 40% reductions in NH_3 and SO_x yield slightly smaller maximum $PM_{2.5}$ decreases of 8.51 μg m^{-3} (10%) and 8.78 μg m^{-3} (9%), respectively. The regional average sensitivities of $PM_{2.5}$ concentrations in East Asia to 40% reductions in individual precursors are ~8% (Fig. 10).

In contrast, $PM_{2.5}$ concentrations in South Asia only show significant responses to SO_x emissions reductions, whilst NH_3 emissions reductions have little effect, which is consistent with our previous finding that South Asia has the most ammonia-rich chemical climate for SIA formation (Ge et al., 2022). The dominant proportion of $(NH_4)_2SO_4$ in SIA compared to NH_4NO_3 in South Asia (Fig. S8) also explains the small sensitivity of $PM_{2.5}$ in this region to NO_x emissions reductions. The maximum $PM_{2.5}$ decrease (7.02 μg m^{-3}, 9%) for 40% SO_x emissions reductions is more than three times larger than the maximum $PM_{2.5}$ decrease (2.20 μg m^{-3}, 4%) for 40% NH_3 emissions reductions. The decreases in regionally averaged $PM_{2.5}$ concentrations in South Asia in response to 40% reductions in emissions of individual precursors are in the order 10% for SO_x, 3% for NO_x, and 1% for NH_3.

In the Euro_Medi region, $PM_{2.5}$ sensitivities vary from north to south. Northern and central Europe is most sensitive to NH_3 and NO_x emissions reductions, for which the maximum decrease in $PM_{2.5}$ is ~2.6 μg m^{-3} (16%) for 40% reductions, while the Mediterranean is more sensitive to SO_x emissions reductions, for which the maximum decrease in $PM_{2.5}$ is 2.98 μg m^{-3} (12%) for 40% reductions. Regionally averaged, however, the $PM_{2.5}$ concentrations in Euro_Medi show comparable sensitivities to the three precursors with decreases in the range 5-8% for 40% emissions reductions in individual precursors.

Over North America, the eastern US shows larger sensitivities of $PM_{2.5}$ to all emissions reduction scenarios than the western US, and reductions in NO_x emissions yield larger decreases in $PM_{2.5}$ than reductions in SO_x and NH_3 emissions. The maximum decrease in $PM_{2.5}$ derived from 40% reductions in NO_x emissions is 3.10 μg m^{-3} (16%); for 40% reductions in NH_3 and SO_x emissions the maximum $PM_{2.5}$ decreases are 2.37 μg m^{-3} (14%) and 1.35 μg m^{-3} (10%) respectively. The regional average sensitivities of $PM_{2.5}$ concentrations in North America to 40% reductions in emissions of individual precursors decreases in a slightly different order: NO_x (8%), SO_x (7%), and NH_3 (4%).

Figure 10 shows that 20% emissions reductions in any precursor lead to decreases in regionally averaged $PM_{2.5}$ concentrations, although the $PM_{2.5}$ sensitivities vary substantially with precursor and region. Given the non-one-to-one chemical responses of SIA components to reductions in emissions in individual precursors discussed in Sect. 3.1, even 20% reductions appear substantial enough to ensure that decreased SIA formation due to decreased precursor emissions dominates over any disbenefits to SIA formation from, for example, increases in oxidant levels induced by NO_x emissions reductions. For instance, 20% reductions in NO_x emissions still cause a decrease of 0.77 μg m^{-3} (3%) in regional average $PM_{2.5}$ in East Asia, despite increasing regional average SO_4^{2-} by 0.10 μg m^{-3} (2%) because it decreases regional average NH_4^+ and fine NO_3^- by greater amounts (0.17 μg m^{-3} (5%) and 0.72 μg m^{-3} (14%) respectively). Similarly, 20% reductions in SO_x emissions decrease regional average $PM_{2.5}$ in East Asia by 1.15 μg m^{-3} (4%) because the decreases in SO_4^{2-} (1.06 μg m^{-3}, 19%) and NH_4^+ (0.32 μg m^{-3}, 9%) caused by reduced $(NH_4)_2SO_4$ formation are larger than the increase in fine NO_3^- (0.20 μg m^{-3}, 4%) due to elevated NH_4NO_3 formation. On the other hand, the mitigation of $PM_{2.5}$ by reducing emissions of all 3 precursors together is impacted by these non-one-to-one chemical responses as well, which causes the net decrease in regional average $PM_{2.5}$ derived from reductions in all 3 precursors to be smaller than the sum of individual $PM_{2.5}$ decreases derived from reductions in emissions of precursors individually. For example, 40% reductions in NH_3, NO_x and SO_x emissions individually decrease regional average $PM_{2.5}$ in East Asia by 2.03 μg m^{-3} (7%), 1.89 μg m^{-3} (7%), and 2.33 μg m^{-3} (8%) respectively (sum of the three: 6.25 μg m^{-3}), while the decrease in regional average $PM_{2.5}$ derived from 40% reduction in all 3 precursors simultaneously is 5.59 μg m^{-3} (20%).

The 40% reduction in emissions of all 3 species yields a maximum decrease in $PM_{2.5}$ of 23.9 μg m^{-3} (25%) over East Asia, followed by 10.4 μg m^{-3} (17%) in South Asia, 5.57 μg m^{-3} (22%) in Euro_Medi, and 5.05 μg m^{-3} (28%) in North America.

The regional average sensitivity of $PM_{2.5}$ concentrations to 20% and 40% reductions in emissions of all 3 species decreases in the order East Asia (10% and 20% for 20% and 40% reductions respectively), Euro_Medi (9% and 17%), North America (8% and 17%), and South Asia (7% and 13%). This trend is related to differences in the contribution of SIA to $PM_{2.5}$ in the different regions. Figure S8 shows the mass contributions of individual $PM_{2.5}$ components to the regional average concentration of $PM_{2.5}$ in the baseline and the 40% emissions reductions scenarios. SIA components in the baseline account for over half of $PM_{2.5}$ in East Asia (52%), followed by Euro_Medi (42%), North America (35%), and South Asia (31%), which explains why reductions in emissions of all three SIA precursors are most efficient for the mitigation of $PM_{2.5}$ in East Asia but least efficient in South Asia. In fact, primary $PM_{2.5}$ is the largest contributor to $PM_{2.5}$ in South Asia, so reducing these emissions will be the most efficient way of abating $PM_{2.5}$ pollution in this region. It is noteworthy that in the scenario of 40% reductions in all 3 species, SIA is still the largest contributor to $PM_{2.5}$ in East Asia, while primary $PM_{2.5}$ and Rest (mainly secondary organic aerosol) become the dominant contributors in other regions. Even with 40% reductions in all three SIA precursors, none of the four regions has its regional average $PM_{2.5}$ concentration decreased to below 5 μg m^{-3}. Euro_Medi (8.4 μg m^{-3} after 40% reductions) and North America (6.5 μg m^{-3}) are the closest, whilst East Asia (21.8 μg m^{-3}) and South Asia (27.0 μg m^{-3}) are still far away from achieving the latest WHO AQG for $PM_{2.5}$. Therefore, reductions in emissions of primary $PM_{2.5}$ and in VOCs are also required to achieve further $PM_{2.5}$ reductions in all regions, or even greater reductions in SIA precursors than simulated here.

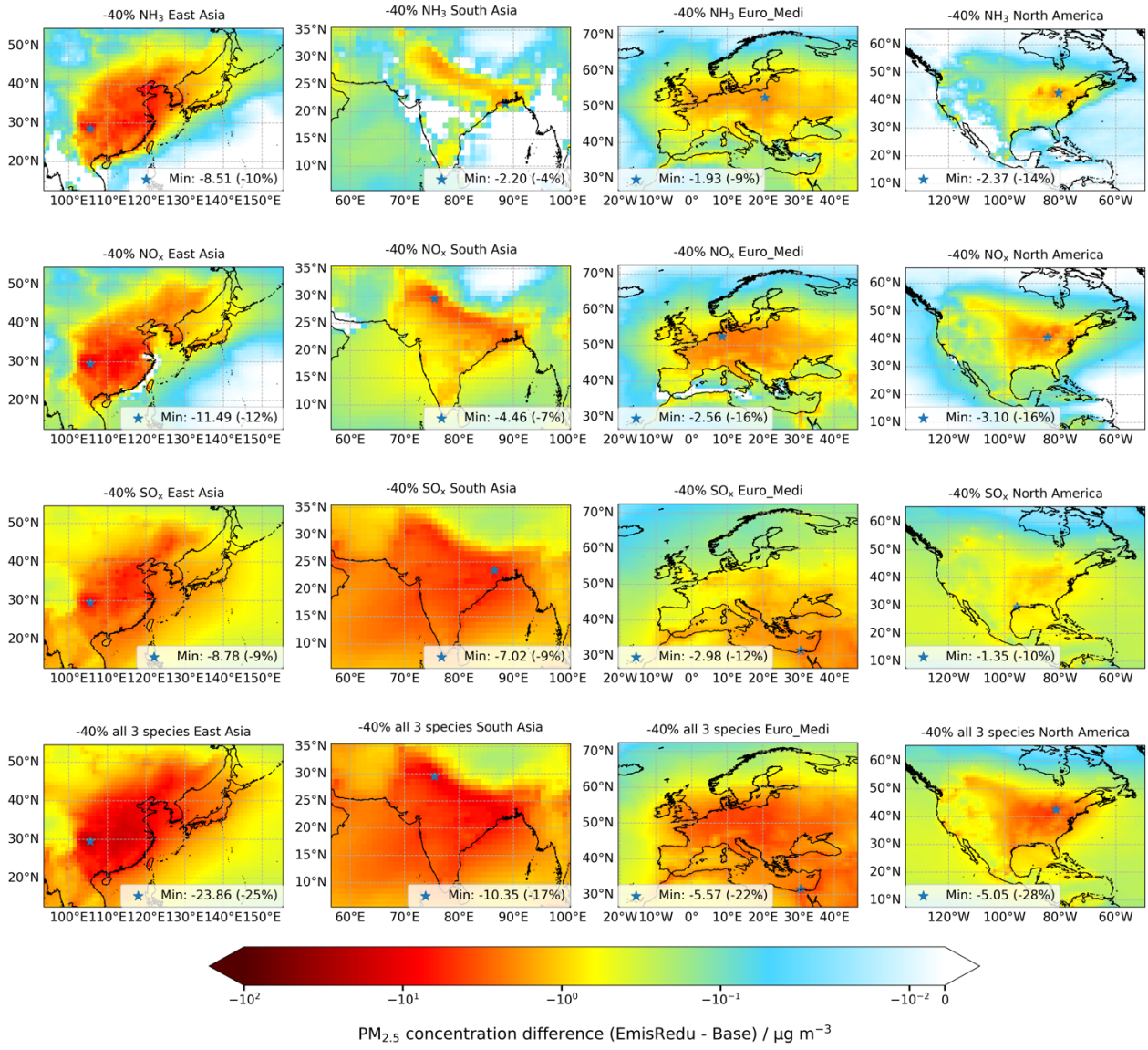

Figure 9: Changes in $PM_{2.5}$ annual mean surface concentrations for 40% emissions reductions in NH_3, NO_x, and SO_x individually and collectively. The blue star in each map locates the minimum difference within each region.

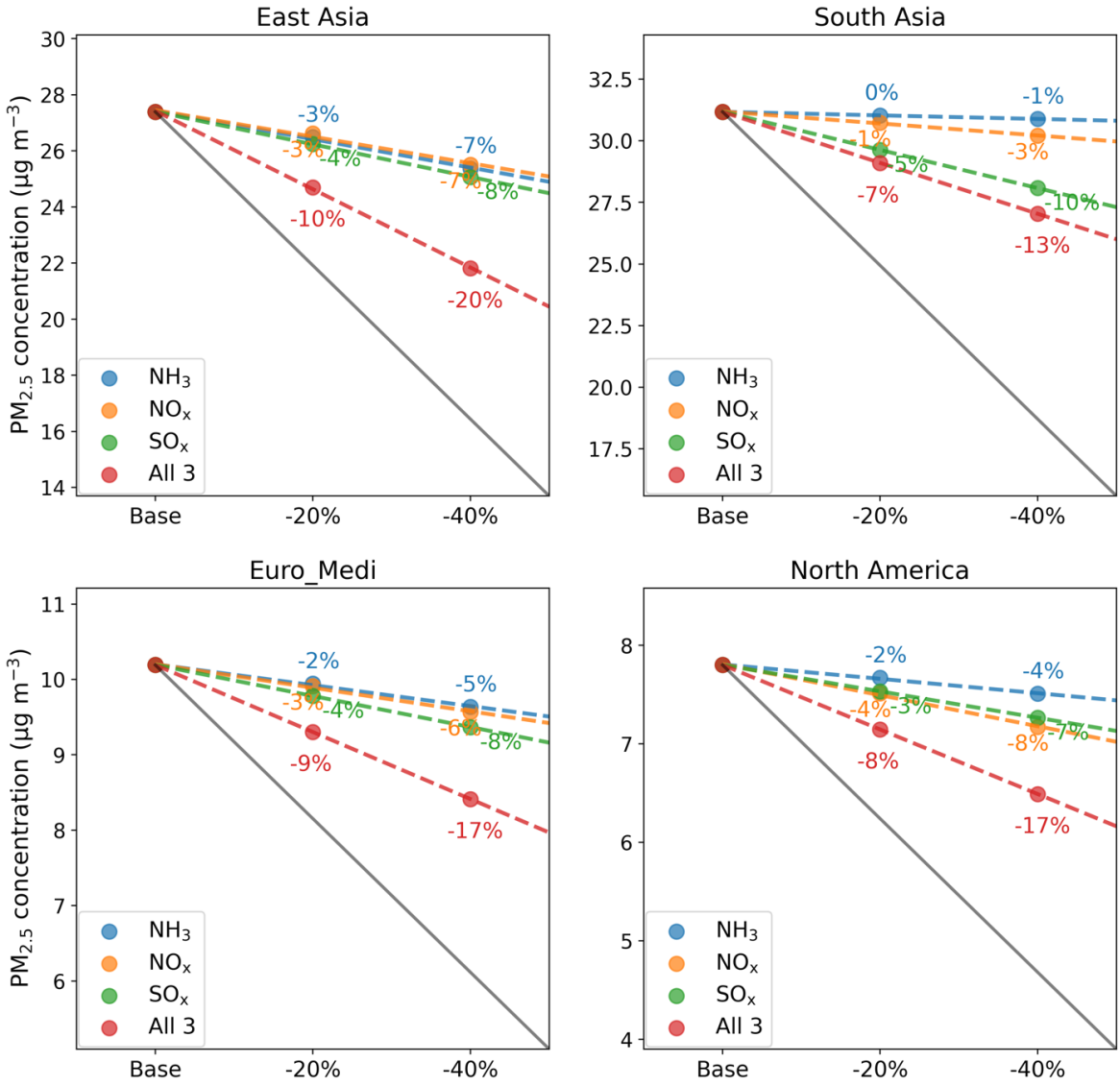

Figure 10: The absolute and relative sensitivities of regionally-averaged annual mean surface concentrations of $PM_{2.5}$ to 20% and 40% emissions reductions in NH_3 (blue), NO_x (orange) and SO_x (green) individually, and collectively (red), for the four regions defined in Fig. 1. The solid grey line in each panel illustrates the one-to-one relative response to emissions reductions, whilst the coloured dashed lines are the linear regressions through each set of three model simulations and illustrate the actual responses to emissions reductions of a given precursor. The numbers show the corresponding relative responses to each emissions reduction (with respect to baseline).

3.3 Sensitivity of N_r and S_r deposition

The impacts of reductions in emissions of NH_3, NO_x and SO_x on total amounts of N and S deposition are straightforward because these must match the emissions mass changes in N and S. However, the relative amounts and spatial pattern of the individual components of N and S deposition are impacted.

Figure 11 shows the spatial variations in the sensitivities of the wet and dry deposition of the RDN components NH_3 and NH_4^+ to 40% reductions in global emissions of NH_3, NO_x, SO_x individually, and collectively. Figure 12 shows similar for deposition of the OXN components NO_x, HNO_3, TNO_3^- (total NO_3^-, the sum of fine and coarse NO_3^-) and Rest (the sum of other oxidized N species). Both wet and dry deposition of NH_3 show negative responses to emissions reductions in NH_3 and all 3 precursors together, but positive responses to emissions reductions in NO_x and SO_x, which is consistent with the responses of surface NH_3 concentrations to these emissions reductions (Sect. 3.1.1). This is because reduced NO_x and SO_x emissions lead to decreased concentrations of acidic species in the atmosphere, resulting in more NH_3 remaining in the gas phase and

485 greater NH_3 deposition over continents. In contrast, global NH_4^+ wet and dry deposition decreases in all emissions reduction scenarios, which is also in line with the decreased NH_4^+ concentrations in all scenarios.

The changes in deposition of the OXN components to emissions reductions are more complicated (Fig. 12). The two species with the largest variation in deposition across the emissions reduction scenarios are HNO_3 and TNO_3^-, which is due to their large contributions to total OXN deposition in most world regions (Ge et al., 2022). For reductions in emissions of NO_x
490 and all 3 species, all OXN deposition components show clear decreasing trends due to the strong reduction in their precursor emissions.

In response to NH_3 emissions reductions, Fig. 12 shows that HNO_3 wet and dry deposition increases in eastern China, northern India, Europe, and eastern North America, whereas the wet and dry deposition of TNO_3^- decreases in these regions. Further examination of fine and coarse NO_3^- deposition differences in Fig. S9 shows that the decrease in TNO_3^- deposition is
495 driven by the decrease in fine NO_3^- wet and dry deposition, while coarse NO_3^- wet and dry deposition in the four regions actually increases. The reduction in NH_3 emissions decreases NH_4NO_3 formation and therefore liberates more HNO_3; as a result, more OXN deposits in the form of HNO_3 rather than NO_3^- in these regions. In contrast, impacts of SO_x emissions reductions on HNO_3 and TNO_3^- deposition are the opposite of impacts of NH_3 emissions reductions. As discussed in Sect. 3.1.2, decreased SO_4^{2-} concentrations promote the formation of NH_4NO_3, which results in decreased wet and dry deposition
500 of HNO_3 and consequently increased TNO_3^- deposition (driven by increased fine NO_3^- deposition, Fig. S9) in eastern China, northern India, Europe, and eastern North America.

Compared to HNO_3 and TNO_3^-, the responses of NO_x and Rest OXN deposition to reductions in NH_3 and SO_x emissions are considerably smaller. For instance, the maximum increases in HNO_3 wet and dry deposition in response to 40% NH_3 emissions reductions are 328 mgN m^{-2} (85%) and 248 mgN m^{-2} (48%) respectively, whereas the maximum increases in Rest
505 OXN wet and dry deposition are only 1.35 mgN m^{-2} (4%) and 1.64 mgN m^{-2} (4%) respectively. Also, in the 40% NH_3 emissions reduction scenario, the maximum decreases in TNO_3^- wet and dry deposition are 359 mgN m^{-2} (25%) and 175 mgN m^{-2} (28%) respectively, whereas the maximum decreases in NO_x dry deposition are only 4.22 mgN m^{-2} (1%).

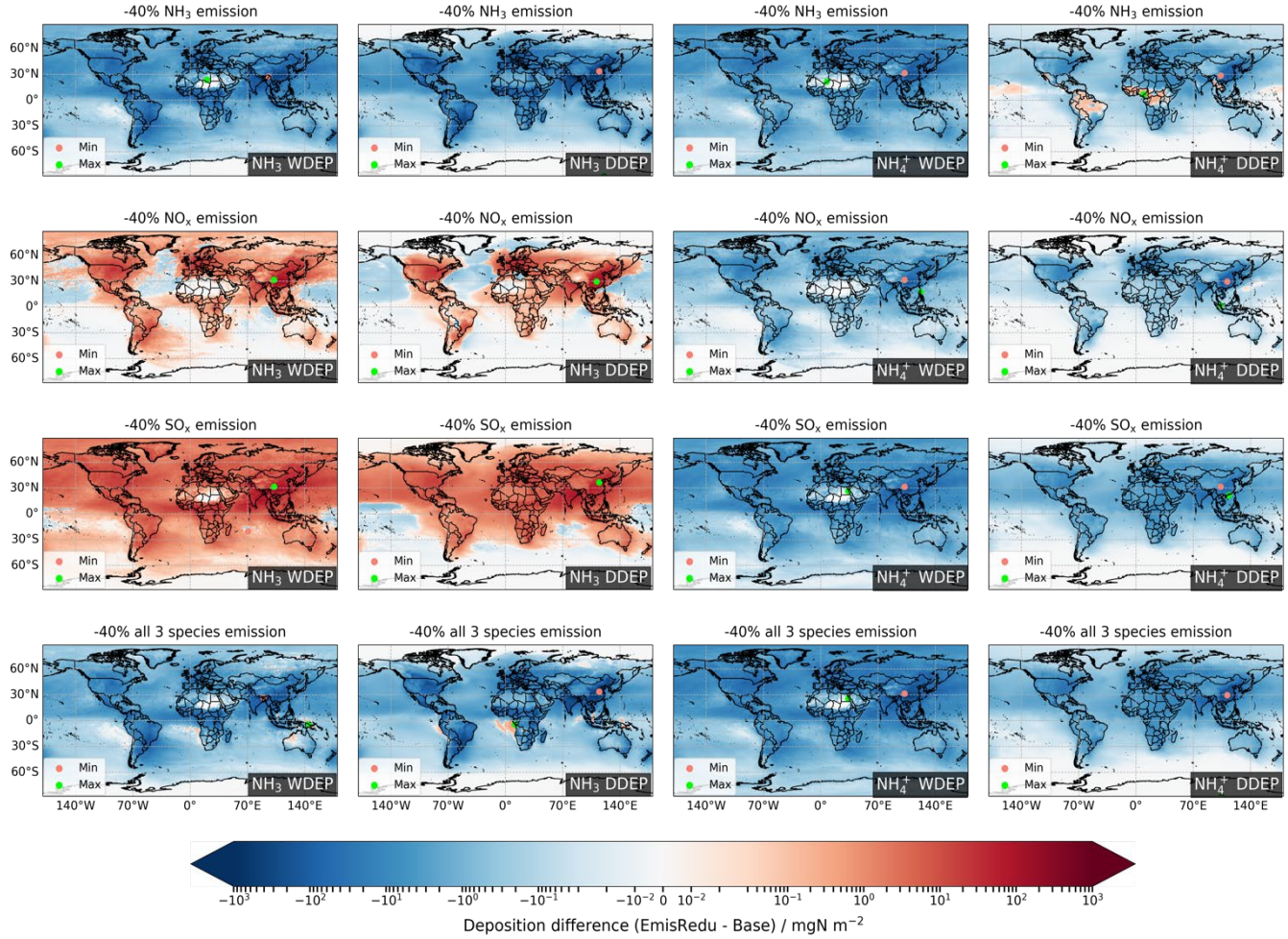

510

Figure 11: Changes in wet (WDEP) and dry deposition (DDEP) of NH_3 and NH_4^+ for 40% emissions reductions in NH_3, NO_x, and SO_x individually and collectively. Red and green dots in each map locate the minimum and maximum difference, respectively.

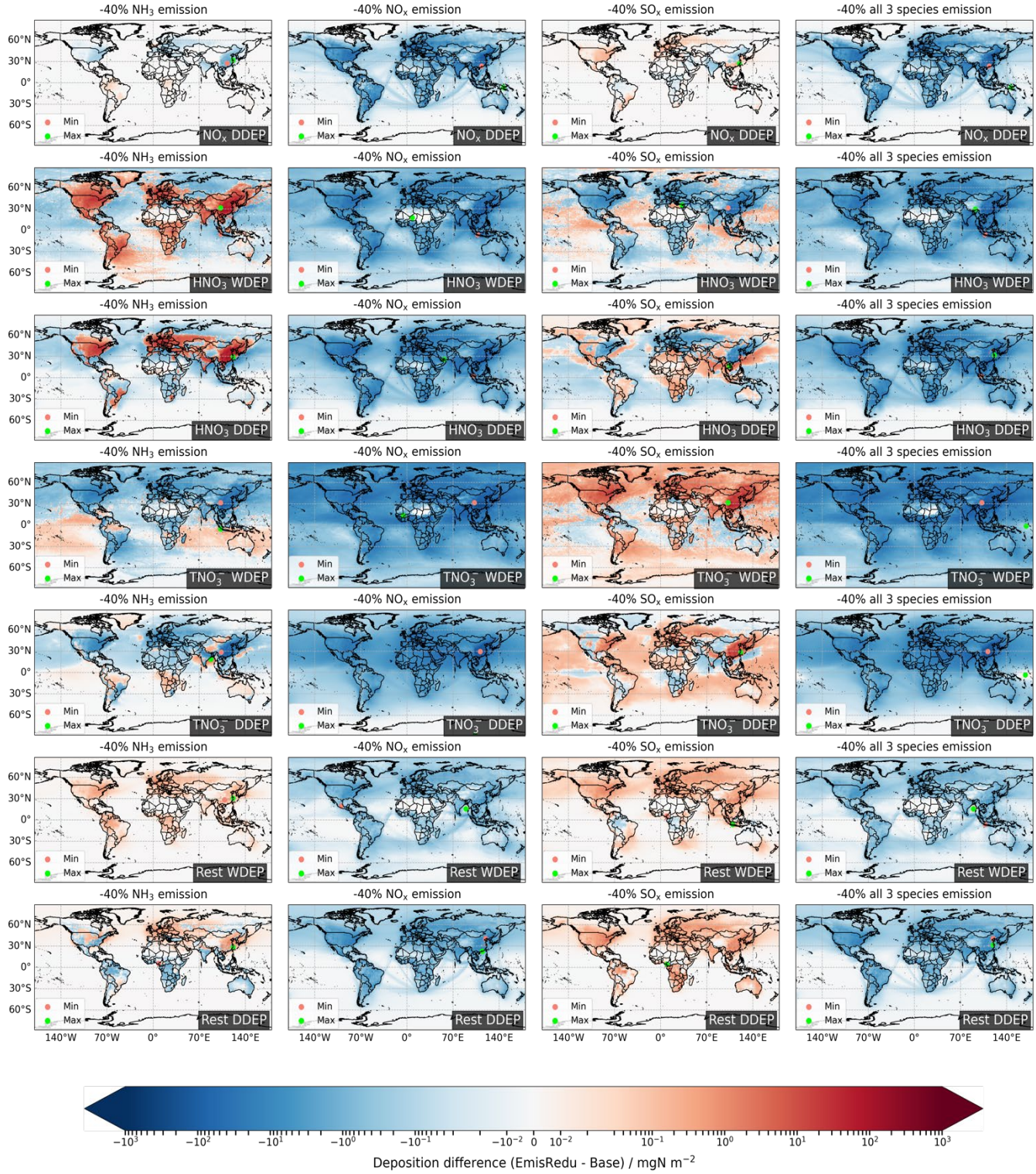

Figure 12: Changes in wet (WDEP) and dry deposition (DDEP) of NO_x, HNO_3, TNO_3^- (fine + coarse NO_3^-), and Rest OXN species for 40% emissions reductions in NH_3, NO_x, and SO_x individually and collectively. Red and green dots in each map locate the minimum and maximum difference, respectively.

The spatial variations in the sensitivities of SO_2 and SO_4^{2-} wet and dry deposition to the precursor emissions reductions are shown in Fig. 13. Increased SO_2 wet deposition is observed globally in response to NH_3 emissions reductions, whilst SO_2 dry deposition decreases over the continents but increases over the oceans. The non-stomatal canopy resistance of SO_2 is positively correlated to the molar acidity ratio a_{SN} (Smith et al., 2000; Erisman et al., 2001; Fowler et al., 2009; Massad et al., 2010; Simpson et al., 2012). Reductions in NH_3 emissions increase the a_{SN}, which therefore increases the canopy resistance

of SO_2 and decreases SO_2 dry deposition over the continents. The 40% reduction in NH_3 emissions yields a global maximum increase in SO_2 wet deposition of 131 mgS m^{-2} (44%), and a maximum decrease in SO_2 dry deposition of 600 mgS m^{-2} (24%). The overall effect of increased SO_2 wet deposition and decreased SO_2 dry deposition is a decreased SO_2 total deposition over populated continents (where NH_3 emissions are high) and increased SO_2 total deposition over oceans (Fig. S5). The maximum decrease of SO_2 total deposition located in southern China is 586 mgS m^{-2} (18%) for 40% NH_3 reduction.

The sensitivity of total deposition of SO_4^{2-} to NH_3 emissions reductions (Fig. S6) follows the trend in the sensitivity of SO_4^{2-} concentrations (Sect. 3.1.3). The responses of wet and dry deposition of SO_4^{2-} to NH_3 emissions reductions are similar (Fig. 13). In general, decreased wet and dry SO_4^{2-} deposition appears over Europe, north-eastern China, and north-eastern US, while increased wet and dry deposition occurs in the rest of the world. As also for their concentration sensitivities, the magnitudes of the SO_4^{2-} deposition responses are much smaller than for SO_2. For 40% NH_3 emissions reduction, the maximum decrease of SO_4^{2-} total deposition is 42 mgS m^{-2} (9%), which is an order of magnitude smaller than that of SO_2 total deposition.

For NO_x emissions reductions, both wet and dry deposition of SO_2 generally show decreases in eastern China, Europe, and north-eastern US but increases in the rest of the world, which is contrary to the responses of SO_4^{2-} wet and dry deposition. This is related to enhanced chemical conversion of SO_2 to SO_4^{2-} due to increased atmospheric oxidizing capacity over eastern China, Europe, and north-eastern US (details in Sect. 3.1.3). The maximum decrease in SO_2 wet and dry deposition in response to 40% reductions in NO_x emissions is ~65 mgS m^{-2}, while the maximum increase in SO_4^{2-} wet and dry deposition is ~50 mgS m^{-2}.

For reductions in SO_x and in all 3 precursors collectively, decreased wet and dry deposition of SO_2 and SO_4^{2-} is observed globally and the 40% reductions in these two scenarios yield similar global maximum decreases in SO_2 deposition (wet: ~937 mgS m^{-2}, 41%; dry: ~1338 mgS m^{-2}, 43%) and SO_4^{2-} deposition (wet: ~828 mgS m^{-2}, 38%; dry: ~150 mgS m^{-2}, 39%).

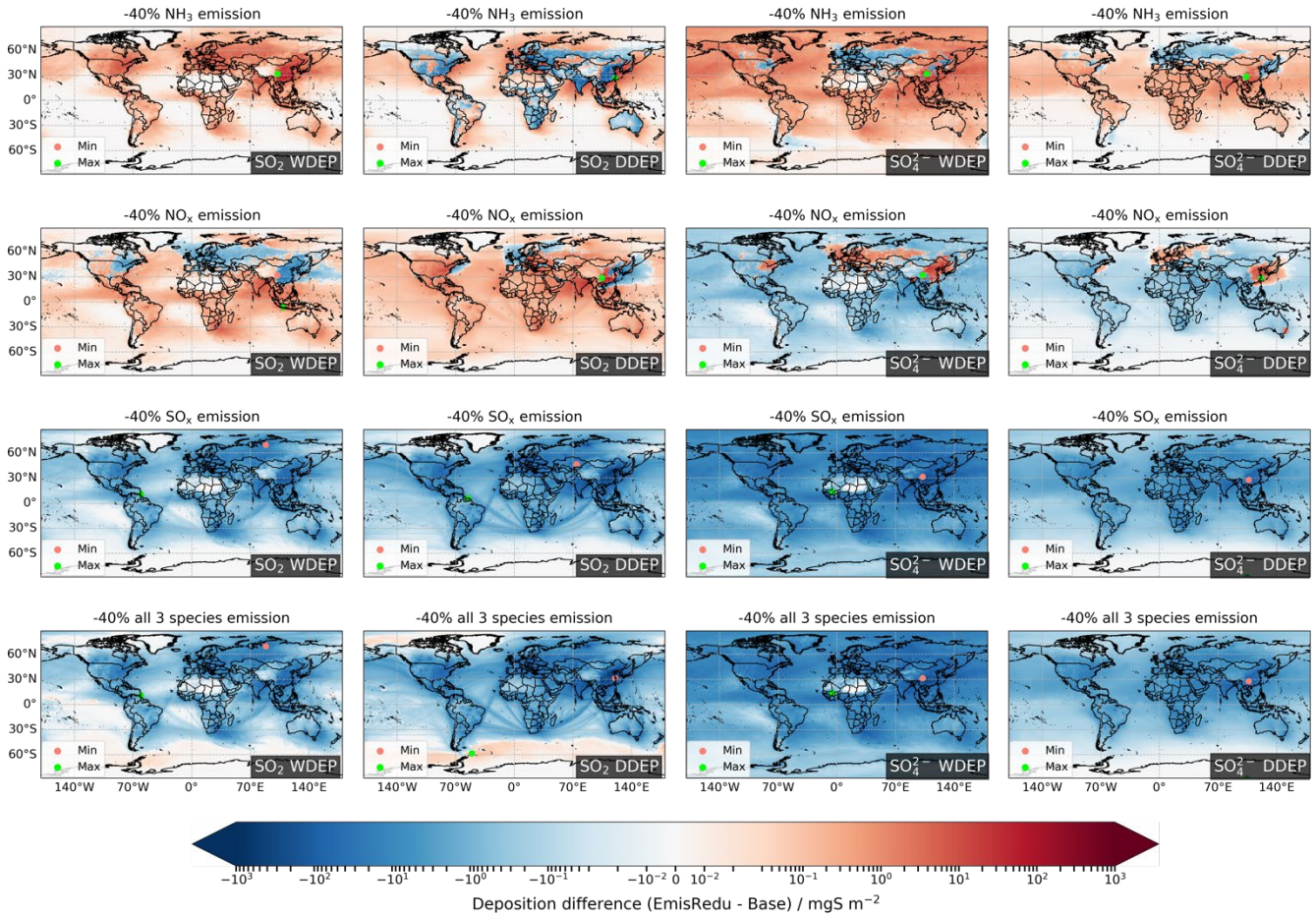

Figure 13: Changes in wet (WDEP) and dry deposition (DDEP) of SO_2 and SO_4^{2-} for 40% emissions reductions in NH_3, NO_x, and SO_x individually and collectively. Red and green dots in each map locate the minimum and maximum difference, respectively.

Figure 14 shows the differences of regional total deposition of individual species between baseline and the 40% emissions reduction scenarios. The regional total RDN, OXN and OXS deposition and the contributions of individual components are listed in Table S6 and S7. As expected, the responses of regional total RDN, OXN and OXS deposition are essentially linear through 20% and 40% reductions in their corresponding precursor, and largely insensitive to reductions in the other precursors, although there are slight differences between regions. For example, 20% and 40% reductions in NH_3 emissions respectively yield 20-21% and 39-41% decreases in total deposition of RDN in the four regions, whilst having no effect on regional total OXN and OXS deposition. The contributions of different deposition components do, however, vary with emission changes and the different lifetimes of the deposition components contribute to the small variabilities in responses of total RDN, OXN and OXS deposition to emissions reductions via differences in the transport through the regional boundaries.

A 40% reduction in NH_3 emissions produces a decrease of 3.58 TgN yr^{-1} (51% of regional total deposition of the same species in baseline; similarly, hereinafter) in NH_3 total deposition and 1.16 TgN yr^{-1} (24%) in NH_4^+ total deposition over East Asia (Fig. 14), which causes the contribution of NH_3 to RDN deposition to decrease from 59% (baseline) to 47% (after 40% NH_3 reduction). In other regions, reductions in NH_3 emissions also decrease NH_3 deposition more effectively than NH_4^+ deposition. Also in East Asia, a 40% NH_3 emissions reduction increases HNO_3 deposition by 0.61 TgN yr^{-1} (20%) and SO_4^{2-} deposition by 0.06 TgS yr^{-1} (2%) but decreases TNO_3^- deposition by 0.55 TgN yr^{-1} (14%) and SO_2 deposition by 0.12 TgS yr^{-1} (3%). As a result, the contribution of HNO_3 deposition to total OXN deposition increases from 30% to 37%, corresponding to a decrease in TNO_3^- contribution from 54% to 47%, whereas changes in contributions of SO_2 and SO_4^{2-} to OXS deposition are very small (Table S7). In other world regions, such changes in total deposition of HNO_3, TNO_3^-, SO_2, and SO_4^{2-} derived from NH_3 emissions reductions are similar but of smaller magnitude.

For 40% NO_x emissions reductions, TNO_3^- deposition shows the largest decrease in East Asia (1.57 TgN yr^{-1}, 35%), South Asia (0.44 TgN yr^{-1}, 26%), and Euro_Medi (0.71 TgN yr^{-1}, 37%), whilst HNO_3 deposition shows the largest decrease in North America (0.56 TgN yr^{-1}, 40%). In contrast, the sensitivities of NO_x dry deposition to NO_x emissions reductions are very small. The contributions of individual OXN deposition components remain fairly constant in all regions. Furthermore, East Asia, Euro_Medi, and North America show a 5% increase in the contribution of NH_3 deposition to total RDN deposition and a corresponding 5% decrease in NH_4^+ contribution for 40% NO_x emissions reductions, which reflects a small shifting of gas-aerosol partitioning for RDN as well. This kind of contribution change in RDN deposition is 2% for South Asia. The impacts of NO_x emissions reductions on OXS deposition compositions are very small.

The 40% reductions in SO_x emissions yield 3.24 TgS yr^{-1} (39%), 1.07 TgS yr^{-1} (38%), 1.17 TgS yr^{-1} (33%), and 0.78 (37%) TgS yr^{-1} decreases in OXS deposition over East Asia, South Asia, Euro_Medi, and North America respectively. SO_x emissions reductions cause larger decreases in SO_2 deposition than in SO_4^{2-} deposition in East Asia and Euro_Medi, while SO_2 and SO_4^{2-} deposition in South Asia and North America show similar sensitivities. This is associated with slightly greater proportions of SO_2 (56-58%) to OXS deposition in the former regions than in the latter regions, and that these proportions are not affected by SO_x emissions reductions (Table S7). NH_3 and NH_4^+ deposition is moderately sensitive to SO_x emissions reductions in the four regions. An increase of 0.75 TgN yr^{-1} (11%) in NH_3 total deposition and a decrease of 0.71 TgN yr^{-1} (14%) in NH_4^+ total deposition for 40% reductions in SO_x emissions is observed over East Asia. For South Asia, Euro_Medi, and North America, the increases in NH_3 total deposition due to 40% SO_x reductions are 0.51 TgN yr^{-1} (12%), 0.25 TgN yr^{-1} (11%), and 0.23 TgN yr^{-1} (12%) respectively. This is because reduced SO_x emissions lead to reductions in $(NH_4)_2SO_4$ formation which then cause increased NH_3 but decreased NH_4^+ concentrations. Another side effect of SO_x emissions reductions in East Asia is a slight decrease in HNO_3 deposition (0.25 TgN yr^{-1}, 10%) and an equivalent increase in TNO_3^- deposition (0.21 TgN yr^{-1}, 5%). The equivalent deposition changes are considerably smaller in the other three regions, which again indicates a larger amount of NH_4NO_3 pollution in East Asia than other regions.

For collective reductions in emissions of all precursors, the changes in deposition of each species reflect net effects of individual reductions in emissions of NH_3, NO_x, and SO_x. For instance, Fig. 14 shows that the decrease in NH_3 deposition in

East Asia derived from 40% reduction in emissions of all 3 species (2.58 TgN yr^{-1}, 36%) is smaller than that from individual NH_3 emissions reduction (3.58 TgN yr^{-1}, 51%) due to the compensating effects of simultaneous NO_x and SO_x emissions reductions in the former scenario. In contrast, the decrease in NH_4^+ deposition in East Asia for 40% emissions reductions in all 3 species (2.11 TgN yr^{-1}, 43%) is almost double that from individual NH_3 emissions reduction scenario (1.16 TgN yr^{-1}, 24%). The variations in chemical forms of RDN, OXN, and OXS deposition affect where they deposit as well since N_r and S_r species have different lifetimes and a shorter lifetime causes a more localised deposition. Many studies show that NH_3 and HNO_3 have shorter lifetimes than NH_4^+ and NO_3^- (Xu and Penner, 2012; Hauglustaine et al., 2014; Bian et al., 2017; Ge et al., 2022). The abatement of total N (TN = RDN + OXN) and S deposition within a certain region is partially offset by this more localised deposition pattern especially in South Asia and Euro_Medi. The 40% reductions in all 3 species emissions yield a 34% (2.93 TgN yr^{-1}) decrease in regional TN deposition in South Asia, and a 34% (1.18 TgS yr^{-1}) decrease in regional OXS deposition in Euro_Medi, which means that less N_r and S_r pollution is transported outside these regions, and more is deposited locally.

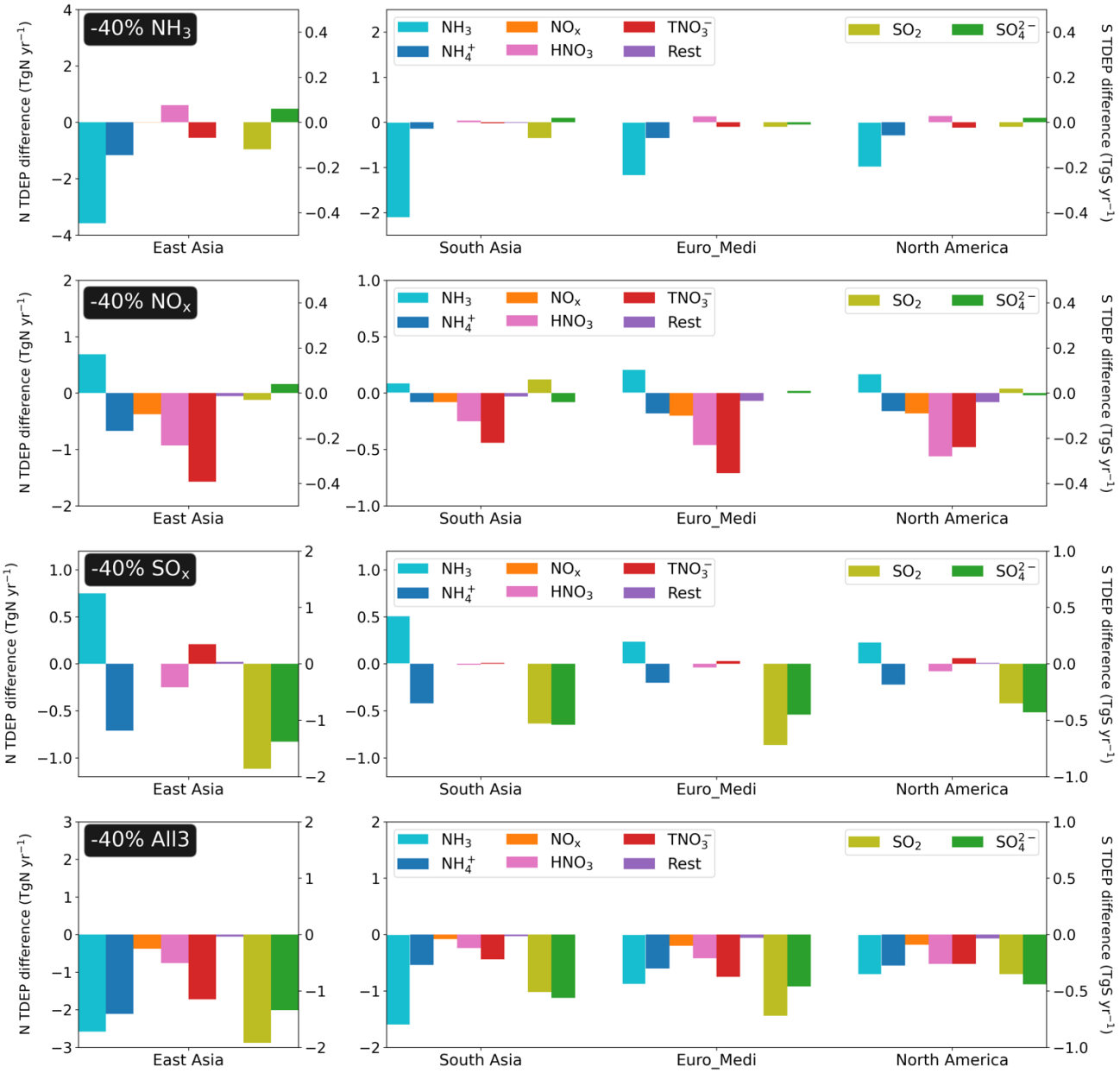

Figure 14: The absolute sensitivities (Emission Reduction - Baseline) of regional total deposition (wet + dry) of NH_3, NH_4^+, NO_x, HNO_3, TNO_3^- (fine + coarse NO_3^-), SO_2 and SO_4^{2-} to 40% emissions reductions in NH_3 (top row), NO_x (2^{nd} row) and SO_x (3^{rd} row) individually, and collectively (bottom row), for the four regions defined in Fig. 1. The left-hand *y* axis in each panel is for RDN and OXN species, while the right-hand *y* axis is for OXS species.

4 Discussions

4.1 Model uncertainty

This study uses global model simulations for 8 emissions reduction scenarios to investigate the geographical variation in the sensitivities of N_r, S_r, and $PM_{2.5}$ to emissions reductions in inorganic precursor gases. Although the EMEP MSC-W ACTM is state-of-the-art and widely used in scientific research and policy development, the analyses presented in this study are based on data from a single modelling system, and their accuracy is therefore subject to any uncertainties in the EMEP MSC-W ACTM's specific parameterisation of atmospheric processes, as well as uncertainties in the chosen emission inventory and meteorology input. However, the evaluation of surface concentrations and wet deposition of N_r and S_r species from this model configuration for the same year against global measurements from 10 monitoring networks (Ge et al., 2021b) has demonstrated the model's capability to capture the overall spatial variations in annual concentrations of NH_3, NH_4^+, NO_2, HNO_3, fine NO_3^-, SO_2 and SO_4^{2-} and their wet deposition in East Asia, Southeast Asia, Europe, and North America. No nationally compiled data for these species is publicly available in Oceania, South Asia, Africa, and Latin America, which inhibits model evaluation in these regions. Similarly, the lack of dry deposition comparison is due to the lack of measurements.

Ge et al. (2021b) also evaluate model outputs derived from two global emission inventories and finds large localised discrepancies in NH_3, NO_2 and SO_2 emissions in certain world regions between the two inventories. The impacts of these discrepancies on modelled concentrations varies with regard to primary or secondary species and differs regionally. Meanwhile, Ge et al. (2021b) indicate that the model shows generally better linear correlations with measurement networks in Southeast Asia ($\bar{R}$ = 0.73 over 7 species), Europe ($\bar{R}$ = 0.67 over 7 species) and North America ($\bar{R}$ = 0.63 over 7 species) than in China ($\bar{R}$ = 0.35 over 5 species), which implies potential discrepancies among different measurements or regional emissions rather than systematic issues with the model parameterisation. The uncertainties in both model and measurement constrains the extent to which the agreement between model and measurement can be used to evaluate a model's performance. The values of statistical metrics for this EMEP-WRF system are at least as good as other global modelling studies (Bian et al., 2017; Hauglustaine et al., 2014). As already indicated, a detailed discussion of model and measurement uncertainties is presented in Ge et al. (2021b).

Additionally, the sensitivities of global and regional N_r, S_r, and $PM_{2.5}$ to various emissions reductions can only be investigated through modelling experiments, and since most model uncertainties will be similar across a set of simulations with the same model configuration, the modelled changes in concentrations between baseline and an emissions reduction scenario should be robust. Nevertheless, considering the fundamental uncertainties in emissions and model parameterizations, all numbers reported in this work should be considered as having underlying uncertainty, albeit that the latest available global emissions inventory and model version were used to minimize the impacts of these uncertainties.

4.2 Regional co-benefits and disbenefits of single-precursor emissions controls

The Results section shows that the reduction in emissions of one individual precursor has multiple co-benefits and sometimes small disbenefits on mitigating N_r, S_r, and $PM_{2.5}$ pollution, and these effects are geographically variable. In this work, our discussion focuses on East Asia, South Asia, Euro_Medi, and North America on account of both the thoroughly evaluated model results and the high population density plus high N_r and S_r pollution in these regions. The comparison of regional responses to emissions reductions reveals differences in regional oxidation regime, SIA chemistry and deposition pattern which are important processes to consider when designing emissions control policies since transitory increases in $PM_{2.5}$ and some N_r and S_r pollutants could occur as emissions reduction measures are gradually applied.

Globally, reductions in NH_3 emissions are effective for reducing NH_3 concentrations and its wet and dry deposition but considerably less effective at reducing NH_4^+. This is because most world regions are in an ammonia-rich chemical domain in which reducing NH_3 emissions only has limited effects on mitigating SIA formation (Ge et al. 2022). Other co-benefits of NH_3

emissions reductions include reductions in fine NO_3^- surface concentrations and deposition in East Asia, South Asia, Euro_Medi, and North America because of reduced NH_4NO_3 formation. A notable disbenefit is the increased SO_2 surface concentration and human exposure in these regions which is caused by reduced SO_2 dry deposition. The dry deposition velocity of SO_2 is negatively correlated with the molar acidity ratio a_{SN} which is a model parameterisation derived from long-term deposition measurements (Erisman et al., 2001; Simpson et al., 2012). Reduced NH_3 emissions therefore increase the acidity, leading to decreased SO_2 dry deposition.

Similarly, whilst reducing NO_x emissions is of course an effective way of decreasing global concentrations and deposition of OXN species, the degree to which different OXN species are decreased varies across regions. A 40% reduction in NO_x emissions decreases NO_x and fine NO_3^- surface concentrations in East Asia by 45% and 33% respectively, whereas in South Asia this measure has a greater effect on fine NO_3^- (45% decrease) than on NO_x (22% decrease). In Euro_Medi and North America, the 40% NO_x emissions reductions produce similar decreases in regional average NO_x (36-38%) and fine NO_3^- (41-42%) concentrations. These varying regional responces are consequent on different regional NO_x oxidation regime and SIA chemistry. The NO_x emissions reductions decrease NO_x surface concentrations, which increases O_3 concentrations in the high NO_x areas of eastern China and western and central Europe and therefore increases the atmospheric oxidizing capacity in these regions. As a result, more SO_2 is oxidized to SO_4^{2-} which leads to decreased SO_2 concentrations and deposition and consequently increased SO_4^{2-} concentrations and deposition in these areas. The enhanced SO_4^{2-} production can partially (or even totally) offset the mass reduction in $PM_{2.5}$ caused by reduced NH_4NO_3 formation when reductions in NO_x emissions are not sufficiently high. The increased oxidant levels will also enhance HNO_3 and NO_3^- production in these regions, but this effect does not compensate for the reduction in HNO_3 and NO_3^- concentrations due to the reductions in their precursors (at least for 20% and 40% NO_x reductions), so the net effect is globally decreased HNO_3 and NO_3^-. Consequently, reduced HNO_3 and NO_3^- levels caused by NO_x emissions reductions lead to less NH_4NO_3 formation, which then results in globally increased NH_3 concentration and deposition and decreased NH_4^+ concentration and deposition. In contrast, decreased O_3 concentrations in South Asia and North America in response to NO_x emissions reductions result in less chemical conversion of SO_2 to SO_4^{2-}, which then causes increased SO_2 and decreased SO_4^{2-} concentrations and deposition. Clappier et al. (2021) and Thunis et al. (2021) showed that the increased atmospheric oxidizing capacity induced by reductions in NO_x emissions is the reason for increased $PM_{2.5}$ levels in the Po basin (Italy) especially during wintertime, with increased nitrate, sulfate and SOA concentrations all being closely related to increased O_3 levels. Balamurugan et al. (2022) reported that reductions in SIA were much smaller than NO_2 emissions reductions during COVID lockdown in Germany, which is because the increased oxidant levels (OH, NO_3 and O_3) enhanced the formation of sulfate and night-time nitrate which then partially offset the lockdown-induced $PM_{2.5}$ decreases. Fu et al. (2020) noted that the increased oxidation of NO_x to HNO_3 due to increased O_3 levels makes winter haze NO_3^- in the North China Plain (NCP) almost insensitive to 30% reductions in emissions of NO_x, while Le et al. (2020) also revealed an unexpected PM exacerbation caused by unfavourable meteorological conditions and intensified SIA formation due to elevated O_3 levels induced by NO_x emissions reductions during COVID lockdown in China.

The greatest effect of SO_x emissions reductions is the direct decrease in global concentrations and deposition of SO_2 and SO_4^2, which then induces changes in gas-aerosol partitioning of NH_3-NH_4^+ and HNO_3-NO_3^-. As discussed above, the reduction in $(NH_4)_2SO_4$ formation frees more gaseous NH_3 and promotes NH_4NO_3 formation, leading to increased concentrations and deposition of NH_3 and fine NO_3^- in all world regions. Considering that one SO_4^{2-} takes up two NH_3 molecules under ammonia-rich conditions, but NO_3^- only takes one, the net effect of SO_x emissions reductions still causes globally decreased NH_4^+ concentrations and deposition. Liu et al. (2018) noted a significant increase in annual NH_3 concentrations caused by rapid SO_2 emissions reductions in the NCP. In addition, the shifting of RDN from aerosol-phase NH_4^+ to gaseous NH_3 in response to reduced SO_x emissions also means that RDN pollution becomes more localized because NH_3 has a much shorter lifetime (1.6 days) than NH_4^+ (8.9 days) as it deposits more quickly to land rather than being transported to other regions (Ge et al. 2022). Utilizing combined measurements and modelling, Leung et al. (2020) found that the reduction in wintertime $PM_{2.5}$ in the NCP

is buffered by enhanced NH_4NO_3 formation due to decreased SO_4^{2-} concentration liberating free NH_3, and increased oxidant levels promoting HNO_3 production, despite SO_2 and NO_x emissions reductions in China. However, it is important to note that $(NH_4)_2SO_4$ has greater molecular mass than NH_4NO_3 and hence has larger leverage on $PM_{2.5}$ mass concentration, which ensures that the reductions in $PM_{2.5}$ mass concentrations derived from reduced $(NH_4)_2SO_4$ are less readily offset by increases in NH_4NO_3 concentrations. This also means that relative changes in the SO_4^{2-} component cause greater mass changes with respect to $PM_{2.5}$ air quality objectives (which must be expressed as mass concentration) than do the same relative changes in the NO_3^- component. The relative changes in the SIA components of $PM_{2.5}$ expressed as molar concentrations would be different.

Additionally, it is noteworthy that changes in SO_x emissions have some subtle effects on NO_x concentrations as well. According to Fig. 4, small increases in NO_x concentrations are observed in southern China, western Europe, and eastern US, while India and north-eastern China show decreased NO_x levels in response to SO_x emissions reductions. These impacts can be attributed to the role of SO_4^{2-} in the hydrolysis of N_2O_5 (which can undergo photolysis and produce NO_2). Many measurement studies, both laboratory and based on ambient samples, have revealed varying rates with different dependencies for this reaction such as the relative humidity, available aerosol surface area, the size and composition of the aerosol particles, and the ratio of sulfate to organic matter (Bertram et al., 2009; Bertram and Thornton, 2009; Chang et al., 2011; Wagner et al. 2013; McDuffie et al. 2018). The parameterization used in the EMEP MSC-W model, based on the work of Riemer et al. (2003), incorporates SO_4^{2-} concentrations (via the parameter of aerosol surface area and reaction probability) into the calculation of the hydrolysis rate of N_2O_5 (Simpson et al. 2012). Consequently, reductions in SO_x emissions affect SO_4^{2-} levels which in turn affect N_2O_5 and NO_x levels. While the changes in NO_x concentrations are small when viewed at a regional average level (0-1%, as depicted in Figure 5), they may be significant in very local areas in the regions mentioned above. This part of the chemistry is one of the most uncertain aspects of the atmospheric science field. As a result, more laboratory and ambient measurement studies are needed to improve and test this type of model parametrization.

4.3 $PM_{2.5}$ sensitivities

This study highlights important messages for policy-makers with respect to regional $PM_{2.5}$ mitigation. The most effective emissions control for decreasing regional average $PM_{2.5}$ concentrations, via an individual component, differs between world regions, as follows.

More emissions controls focusing on NH_3 and NO_x are necessary for regions with better air quality such as Europe and North America to decrease the annual $PM_{2.5}$ concentrations below the latest WHO guideline of 5 μg m^{-3} (WHO, 2021). More specifically, $PM_{2.5}$ sensitivities in Euro_Medi are complex and vary from the north to south. The UK and Scandinavia are more sensitive to NH_3 emissions reductions, central Europe is more sensitive to NO_x, while the Mediterranean region is more sensitive to SO_x, which is consistent with conclusions from other European studies (Megaritis et al., 2013; Vieno et al., 2016; Aksoyoglu et al., 2020; Jiang et al., 2020; Clappier et al., 2021). From a perspective of Europe-wide policy making, it is important to reduce NH_3 and NO_x emissions together and/or go for stronger reductions to minimise adverse effects caused by enhanced oxidation efficiency. In North America, the most effective measure to decrease annual mean $PM_{2.5}$ is reducing NO_x emissions. Similar conclusions are reported by other studies. Liao et al. (2008) reported that the reduction in NO_x emissions was most effective for decreasing 24-h mean $PM_{2.5}$ levels for five cities in the US, while Kelly et al. (2021) reported that reducing NO_x emissions was more effective for reducing $PM_{2.5}$ concentrations in the eastern US than SO_2, NH_3, and VOC emissions reductions in both January and July. Tsimpidi et al. (2007, 2008) showed that NO_x emissions reductions were the most effective measure for controlling $PM_{2.5}$ in the eastern US in summer due to the combined effects of lower atmospheric oxidant levels and smaller precursor emissions. Unfortunately, no conclusion on annual mean $PM_{2.5}$ sensitivities was drawn from these studies.

$PM_{2.5}$ in South Asia is most sensitive to SO_x emissions reductions, and least sensitive to NH_3 emissions reductions, which is because South Asia is extremely ammonia-rich (Ge et al., 2022) so reducing NH_3 has little impact on mitigating SIA. In this study, 40% reductions in SO_x and NH_3 emissions respectively produce 10% and 1% decreases in South Asia regional average $PM_{2.5}$. Pozzer et al. (2017) also showed that NH_3 emissions control has negligible impacts on $PM_{2.5}$ levels in South Asia with a 50% reduction in NH_3 emissions only reducing annual mean $PM_{2.5}$ by 2%. Given the continuing strong growth of SO_2 emissions in India now and in future projections (Sadavarte and Venkataraman, 2014; Hoesly et al., 2018; Aas et al., 2019; Szopa et al., 2021), it is anticipated that $PM_{2.5}$ levels in this region will continue to rise.

For East Asia, although considerable emissions reductions in SO_2 have been taking place in China, and to a lesser extent reductions in NO_x (Liu et al., 2016; Hoesly et al., 2018; Zheng et al., 2018), continuous efforts need to be put into reducing not only SO_2 and NO_x but also NH_3 as reductions in the three precursors are equally effective for mitigating $PM_{2.5}$. Studies focusing on East Asia also highlight the importance of NH_3 emissions control for reducing annual $PM_{2.5}$ pollution especially in central and eastern China (Wang et al., 2011; Pozzer et al., 2017; Cheng et al., 2021). In addition, due to the high proportion of SIA in $PM_{2.5}$ in East Asia, reducing all 3 precursors together also produces the greatest reduction in regional average $PM_{2.5}$ compared to South Asia, Europe, and North America. Another benefit of collective emissions reductions is that it minimises the adverse side effects from individual reductions since these disbenefits can cause transitory increases in $PM_{2.5}$ and deposition of certain N_r and S_r species when emission reduction measures are gradually applied.

In short, considering the evolution of the chemical state of the atmosphere in Europe and North America since the industrial revolution, the measures to combat $PM_{2.5}$ pollution in the two regions may be a good reference for countries in East and South Asia.

4.4 Non-one-to-one linearity

Analyses of both 20% and 40% emissions reductions reveal different kinds of linearity and non-linearity. There is considerable non-linearity in the sense of a lack of one-to-one proportionality between an emission reduction and a species concentration or deposition change. Precursor emissions reduction sometimes even increases other pollutant concentrations. This is consequent on interactions in SIA formation, atmospheric oxidizing capacity, and N and S deposition as discussed earlier, and is highly geographically variable. Such non-one-to-one proportionality may be more significant in a certain area during a certain season due to the inter-annual variability in local meteorology and emissions profiles. However, whilst the sensitivity of an annual quantity of a pollutant to emissions reductions is subject to seasonality, we are confident that the broad conclusions of this study will hold, and from a global and regional policymaking perspective, it is more practical to develop policies of reductions in emissions from different sectors and countries on an annual level. Studies focusing on non-proportional responses of European $PM_{2.5}$ to emissions reductions showed that significant seasonality only occurs in a few specific areas (Thunis et al., 2015, 2021; Clappier et al., 2021).

On the other hand, a linearity in response to emissions reductions is apparent via the observation that the responses of $PM_{2.5}$, N_r, and S_r annual concentrations and deposition components remain essentially proportional to the precursor emissions reductions (20% and 40%) for a given precursor in a given region, albeit that the magnitude of the slope varies substantially with different precursors and regions. Even if the net concentration changes of one species (e.g., $PM_{2.5}$) induced by reductions in emissions of all 3 precursors are smaller (or greater) than the sum of changes from reductions in individual precursors due to different chemical interactions as discussed earlier, these net changes still follow a very similar gradient when emissions reductions in all 3 precursors change from 20% to 40%. However, where the gradient in the response is not one-to-one, the linearity in the response that is observed up to the 40% emissions reductions simulated here clearly cannot continue to extrapolate linearly all the way to 100% emissions reductions. The gradient of the response must be flatter or steeper (depending on atmospheric component) at the beginning or end of the span from zero to 100% emissions reduction. For instance, 20% and 40% reductions in NH_3 emissions give 24% and 48% decreases in global annual mean NH_3 concentrations

respectively (i.e., gradients exceeding one-to-one), whereas these emissions reductions only produce 6% and 14% decreases in global NH_4^+ concentrations, respectively (i.e., gradients less than one-to-one). When NH_3 emissions are completely switched off, both NH_3 and NH_4^+ concentrations will be zero, so the NH_3 concentration sensitivity must become smaller, and the NH_4^+ concentration sensitivity must become larger, as NH_3 emissions reductions approach 100%. Additional serial sensitivity experiments are required to acquire the full spectrum of NH_3 and NH_4^+ (and all other species) sensitivities. It is therefore important for policy-makers in different regions to know the emissions reductions required to obtain the mitigation responses needed for specific air quality targets.

4.5 Implications and limitations

The parameterisation of atmospheric processes in ACTMs is in continuous interplay with the experimental evidence. The responses of N_r and S_r species to emissions reductions in NH_3, NO_x and SO_x as discussed in previous sections reveal several complex processes incorporated in the EMEP MSC-W model. The extent to which these parameterised processes accurately represent the reality of the atmosphere calls for more experimental evidence (field and/or laboratory measurements).

For instance, the synergistic interaction between NH_3 and SO_2 dry deposition to leaf surfaces is well known and has been termed 'co-deposition'. The idea is that the existence of both NH_3 and SO_2 acts to reduce the canopy resistances and increase the dry deposition rate for both gases (Sutton et al., 1994; Fowler et al., 2001; Nemitz et al., 2004; Fowler et al., 2009; Massad et al., 2010). This co-deposition effect is incorporated into the EMEP MSC-W model, making use of empirical parameters derived from European field measurements (Erisman et al., 2001) which may not be completely applicable to other world regions (e.g., South America). In addition, for regional variations in atmospheric oxidizing capacity caused by NO_x emissions reductions, there are several studies reporting measurements evidence in East Asia, Europe, and North America, while no such measurements are found in South Asia. Long-term standardised measurements for both surface concentrations and wet and dry deposition with a sufficient amount of sampling sites in each geographical region are required for corroborating globally modelled results. The quantitative results reported in this study can serve as a reference for future modelling and measurement studies, albeit firmer field evidence worldwide is required to develop a reliable and robust chemistry and deposition schemes for global models.

Finally, it is also important to remember that reductions in anthropogenic emissions of SIA precursors will have many co-benefits on forest health, ecosystem biodiversity, and climate, not just in populated areas but elsewhere. For instance, NH_3 has become a major air pollution driver of lichen distributions in many European forests in recent years. In Scotland, Sutton et al. (2009) showed how lichens were gradually eradicated in areas near a poultry farm which is a large emitter of NH_3. Similarly, van Herk. (2001) reported that increased ambient NH_3 concentrations in the Netherlands appear to be the primary cause of the disappearance of acidophytic lichen species (i.e., species that prefer naturally acidic bark) over the last decade. Moreover, although the effects on the availability of nutrients in terrestrial and aquatic ecosystems are broadly assumed to be decided by total N inputs, Sutton et al. (2020) placed a stronger emphasis on the form in which the N was deposited. In their experiments, dry deposition of NH_3 showed a larger toxicity than wet deposition of NH_4^+ and NO_3^-. In this case, policy-makers should be more cautious about emissions controls with side effects of increased NH_3 dry deposition. Meanwhile, since most NH_3 is emitted via volatilization, a warmer atmosphere will promote its global emissions (Johnson et al. 2008; Sutton et al. 2013; Riddick et al. 2018). NH_3 emission controls thus need to include both direct reductions and indirect measures to abate climate warming as well.

5 Conclusions

The sensitivities of global and regional annual mean surface concentrations and deposition of gaseous and particle N_r and S_r to 20% and 40% reductions in anthropogenic emissions of NH_3, NO_x, and SO_x both individually and collectively has been investigated using the EMEP MSC-W model coupled with WRF meteorology for 2015. East Asia, South Asia, Euro_Medi, and North America are selected for regional discussions because of their high population densities and N_r and S_r pollution, and because the model outputs are evaluated and agree reasonably well with measurements in most of these areas. The comparison in regional responses reveals that the emissions reduction in one precursor has multiple co-benefits and sometimes small disbenefits on mitigating N_r, S_r, and $PM_{2.5}$ pollution, and these effects are highly geographically variable.

Whilst reductions in NH_3 emissions are effective for decreasing annual NH_3 concentrations and deposition they are considerably less effective at decreasing NH_4^+. This is because all densely populated continents are ammonia-rich so reducing NH_3 emissions only has limited effects on mitigating SIA formation. A 40% reduction in NH_3 emissions decreases regional average NH_3 concentrations in the four regions by 47-49%, while NH_4^+ concentrations decrease in the order Euro_Medi (18%), East Asia (15%), North America (12%), and South Asia (4%), the order of increasing regional ammonia-richness. A notable disbenefit is increased SO_2 concentrations because reduced NH_3 levels affect the pH-dependent SO_2 dry deposition. A 40% reduction in NH_3 emissions increases SO_2 concentrations in East Asia by 16%, in South Asia and North America by 14%, and in Euro_Medi by 10%.

Large regional differences are observed in NO_x emissions reduction scenarios. In East Asia, NO_x concentrations are very effectively decreased (by 45%) with 40% NO_x emissions reductions, but they are less effectively decreased in Euro_Medi (38%) and North America (36%), and to a least extent in South Asia (22%). By contrast, the regional sensitivities of fine NO_3^- are reversed: South Asia shows the largest decrease (45%), whilst East Asia shows the smallest decrease (33%). This phenomenon is related to different regional oxidation regime and SIA chemistry. NO_x emissions reductions increase O_3 levels in East Asia (and also, but by less, in Euro_Medi), but decrease O_3 levels in South Asia (and also, but by less, in North America), which causes an enhanced NO_x and SO_x oxidation in former regions but a decreased one in latter regions. Consequently, increased SO_4^{2-} and SO_2 concentrations appear in East Asia and South Asia respectively.

Reductions in SO_x emissions have globally consistent impacts on SO_2 and SO_4^{2-} concentrations. A 40% reduction in SO_x emissions decreases SO_2 and SO_4^{2-} concentrations in the four regions by 42-45% and 34-38% respectively, while the disbenefit is that decreased $(NH_4)_2SO_4$ formation yields ~12% growth in NH_3 total deposition.

This work also highlights important messages for policy-makers concerning the mitigation of $PM_{2.5}$. More emissions controls focusing on NH_3 and NO_x are necessary for regions with better air quality such as Europe and North America. In Euro_Medi, $PM_{2.5}$ sensitivities vary from the north to south, with NH_3 reductions being more effective for UK and Scandinavia, NO_x for central Europe, and SO_x for the Mediterranean. In South Asia, $PM_{2.5}$ is most sensitive to SO_x, and least sensitive to NH_3, which is consistent with the fact that South Asia is so ammonia-rich that reducing NH_3 hardly has any impacts. Given the continuing strong growth of SO_2 emissions in India now and in future projections, it is anticipated that $PM_{2.5}$ levels in this region will continue to rise. In East Asia, although considerable emissions reductions in SO_2 have been taking place in China, and to a lesser extent reductions in NO_x also, continuing efforts need to be put into reducing not only SO_2 and NO_x but also NH_3 as reductions in the three precursors are equally effective for mitigating $PM_{2.5}$.

This work reveals some geographically-varying and non-one-to-one proportionality of chemical responses of N_r, S_r, and $PM_{2.5}$ to emissions reductions. It is thus important not only to prioritise different emission controls in different regions, but also to reduce several emissions together in order to minimise the potential disbenefits.

Code and data availability

As described and referenced in Sect. 2 of this paper, this study used two open-source global models: the European Monitoring and Evaluation Programme Meteorological Synthesizing Centre – West atmospheric chemistry transport model (EMEP MSC-W, 2020, version 4.34, source code available at https://doi.org/10.5281/zenodo.3647990, last access: 18 January 2023) and the Weather Research and Forecasting meteorological model (WRF, version 3.9.1.1, https://www.wrf-model.org, last access: 8 Aug 2022; Skamarock et al., 2008). The model outputs presented in figures and tables in this paper and the corresponding Python scripts are available at https://doi.org/10.5281/zenodo.7082661, last access: 18 January 2023 (Ge, 2022).

Author contribution

MH, DS and MV conceptualised and supervised the study. MV and PW contributed to model development and set-up and provided modelling support. MV provided computing resource. YG contributed to study design, undertook all model simulations, formal data analyses, visualisation of the results and data curation, with discussion and refinement by all authors. The original draft of the paper was written by YG with contributions and editing by MH. All authors provided review comments and approval of the final version.

Competing interests

The authors declare that they have no conflict of interest.

Acknowledgments

Y. Ge gratefully acknowledges studentship funding from the University of Edinburgh and its School of Chemistry. This work was in part supported by the UK Natural Environment Research Council (NERC), including grant nos. NE/R016429/1 and NE/R000131/1, the Department for Environment, Food and Rural Affairs (Defra) contract "Research & Development Support for National Air Pollution Control Strategies (ECM: 62041) 2021 to 2024", and the European Modelling and Evaluation Programme under the United Nations Economic Commission for Europe Convention on Long-range Transboundary Air Pollution.

References

Aas, W., Mortier, A., Bowersox, V., Cherian, R., Faluvegi, G., Fagerli, H., Hand, J., Klimont, Z., Galy-Lacaux, C., Lehmann, C. M. B., Myhre, C. L., Myhre, G., Olivié, D., Sato, K., Quaas, J., Rao, P. S. P., Schulz, M., Shindell, D., Skeie, R. B., Stein, A., Takemura, T., Tsyro, S., Vet, R., and Xu, X.: Global and regional trends of atmospheric sulfur, Scientific Reports, 9, 953, 10.1038/s41598-018-37304-0, 2019.

Aksoyoglu, S., Jiang, J., Ciarelli, G., Baltensperger, U., and Prévôt, A. S. H.: Role of ammonia in European air quality with changing land and ship emissions between 1990 and 2030, Atmos. Chem. Phys., 20, 15665-15680, 10.5194/acp-20-15665-2020, 2020.

AQEG: Mitigation of United Kingdom PM2.5 Concentrations, Air Quality Expert Group, UK Department for Environment, Food and Rural Affairs, London, PB13837, available at: https://uk-air.defra.gov.uk/assets/documents/reports/cat11/1508060903_DEF-PB14161_Mitigation_of_UK_PM25.pdf, 2015.

Balamurugan, V., Chen, J., Qu, Z., Bi, X., and Keutsch, F. N.: Secondary PM2.5 decreases significantly less than NO2 emission reductions during COVID lockdown in Germany, Atmos. Chem. Phys., 22, 7105-7129, 10.5194/acp-22-7105-2022, 2022.

Behera, S. N., Sharma, M., Aneja, V. P., and Balasubramanian, R.: Ammonia in the atmosphere: a review on emission sources, atmospheric chemistry and deposition on terrestrial bodies, Environmental Science and Pollution Research, 20, 8092-8131, https://doi.org/10.1007/s11356-013-2051-9, 2013.

Berge, E., and Jakobsen, H. A.: A regional scale multilayer model for the calculation of long-term transport and deposition of air pollution in Europe, Tellus B: Chemical and Physical Meteorology, 50, 205-223, 10.3402/tellusb.v50i3.16097, 1998.

Bergström, A.-K., and Jansson, M.: Atmospheric nitrogen deposition has caused nitrogen enrichment and eutrophication of lakes in the northern hemisphere, Global Change Biology, 12, 635-643, https://doi.org/10.1111/j.1365-2486.2006.01129.x, 2006.

Bergström, R., Hallquist, M., Simpson, D., Wildt, J., and Mentel, T. F.: Biotic stress: a significant contributor to organic aerosol in Europe?, Atmos. Chem. Phys., 14, 13643-13660, 10.5194/acp-14-13643-2014, 2014.

Bertram, T. H., and Thornton, J. A.: Toward a general parameterization of N2O5 reactivity on aqueous particles: the competing effects of particle liquid water, nitrate and chloride, Atmos. Chem. Phys., 9, 8351-8363, 10.5194/acp-9-8351-2009, 2009.

Bertram, T. H., Thornton, J. A., Riedel, T. P., Middlebrook, A. M., Bahreini, R., Bates, T. S., Quinn, P. K., and Coffman, D. J.: Direct observations of N2O5 reactivity on ambient aerosol particles, Geophysical Research Letters, 36, https://doi.org/10.1029/2009GL040248, 2009.

Bian, H., Chin, M., Hauglustaine, D. A., Schulz, M., Myhre, G., Bauer, S. E., Lund, M. T., Karydis, V. A., Kucsera, T. L., Pan, X., Pozzer, A., Skeie, R. B., Steenrod, S. D., Sudo, K., Tsigaridis, K., Tsimpidi, A. P., and Tsyro, S. G.: Investigation of global particulate nitrate from the AeroCom phase III experiment, Atmospheric Chemistry and Physics, 17, 12911-12940, 10.5194/acp-17-12911-2017, 2017.

Botha, C. F., Hahn, J., Pienaar, J. J., and Van Eldik, R.: Kinetics and mechanism of the oxidation of sulfur(IV) by ozone in aqueous solutions, Atmospheric Environment, 28, 3207-3212, https://doi.org/10.1016/1352-2310(94)00174-J, 1994.

Brauer, M., Freedman, G., Frostad, J., van Donkelaar, A., Martin, R. V., Dentener, F., Dingenen, R. v., Estep, K., Amini, H., Apte, J. S., Balakrishnan, K., Barregard, L., Broday, D., Feigin, V., Ghosh, S., Hopke, P. K., Knibbs, L. D., Kokubo, Y., Liu, Y., Ma, S., Morawska, L., Sangrador, J. L. T., Shaddick, G., Anderson, H. R., Vos, T., Forouzanfar, M. H., Burnett, R. T., and Cohen, A.: Ambient Air Pollution Exposure Estimation for the Global Burden of Disease 2013, Environmental Science & Technology, 50, 79-88, 10.1021/acs.est.5b03709, 2016.

Chang, M., Cao, J., Ma, M., Liu, Y., Liu, Y., Chen, W., Fan, Q., Liao, W., Jia, S., and Wang, X.: Dry deposition of reactive nitrogen to different ecosystems across eastern China: A comparison of three community models, Science of The Total Environment, 720, 137548, https://doi.org/10.1016/j.scitotenv.2020.137548, 2020.

Chang, W. L., Bhave, P. V., Brown, S. S., Riemer, N., Stutz, J., and Dabdub, D.: Heterogeneous Atmospheric Chemistry, Ambient Measurements, and Model Calculations of N2O5: A Review, Aerosol Science and Technology, 45, 665-695, 10.1080/02786826.2010.551672, 2011.

Chen, C., Zhu, P., Lan, L., Zhou, L., Liu, R., Sun, Q., Ban, J., Wang, W., Xu, D., and Li, T.: Short-term exposures to PM2.5 and cause-specific mortality of cardiovascular health in China, Environmental Research, 161, 188-194, https://doi.org/10.1016/j.envres.2017.10.046, 2018a.

Chen, L., Shi, M., Gao, S., Li, S., Mao, J., Zhang, H., Sun, Y., Bai, Z., and Wang, Z.: Assessment of population exposure to PM2.5 for mortality in China and its public health benefit based on BenMAP, Environmental Pollution, 221, 311-317, https://doi.org/10.1016/j.envpol.2016.11.080, 2017.

Chen, X., Wang, Y.-h., Ye, C., Zhou, W., Cai, Z.-c., Yang, H., and Han, X.: Atmospheric Nitrogen Deposition Associated with the Eutrophication of Taihu Lake, Journal of Chemistry, 2018, 4017107, 10.1155/2018/4017107, 2018b.

Cheng, L., Ye, Z., Cheng, S., and Guo, X.: Agricultural ammonia emissions and its impact on PM2.5 concentrations in the Beijing–Tianjin–Hebei region from 2000 to 2018, Environmental Pollution, 291, 118162, https://doi.org/10.1016/j.envpol.2021.118162, 2021.

Ciarelli, G., Theobald, M. R., Vivanco, M. G., Beekmann, M., Aas, W., Andersson, C., Bergström, R., Manders-Groot, A., Couvidat, F., Mircea, M., Tsyro, S., Fagerli, H., Mar, K., Raffort, V., Roustan, Y., Pay, M. T., Schaap, M., Kranenburg, R., Adani, M., Briganti, G., Cappelletti, A., D'Isidoro, M., Cuvelier, C., Cholakian, A., Bessagnet, B., Wind, P., and Colette, A.: Trends of inorganic and organic aerosols and precursor gases in Europe: insights from the EURODELTA multi-model experiment over the 1990–2010 period, Geoscientific Model Development, 12, 4923-4954, 10.5194/gmd-12-4923-2019, 2019.

Clappier, A., Thunis, P., Beekmann, M., Putaud, J. P., and de Meij, A.: Impact of SOx, NOx and NH3 emission reductions on PM2.5 concentrations across Europe: Hints for future measure development, Environment International, 156, 106699, https://doi.org/10.1016/j.envint.2021.106699, 2021.

Crippa, M., Solazzo, E., Huang, G., Guizzardi, D., Koffi, E., Muntean, M., Schieberle, C., Friedrich, R., and Janssens-Maenhout, G.: High resolution temporal profiles in the Emissions Database for Global Atmospheric Research, Scientific Data, 7, 121, 10.1038/s41597-020-0462-2, 2020.

EEA: Air quality in Europe – 2021 report. EEA Report No. 15/2021., European Environment Agency, Publications Office of the European Union, available at: https://www.eea.europa.eu/publications/air-quality-in-europe-2021/ (last access: 7 August 2022), 2021.

Erisman, J. W., Hensen, A., Fowler, D., Flechard, C. R., Grüner, A., Spindler, G., Duyzer, J. H., Weststrate, H., Römer, F., Vonk, A. W., and Jaarsveld, H. v.: Dry Deposition Monitoring in Europe, Water, Air and Soil Pollution: Focus, 1, 17-27, 10.1023/A:1013105727252, 2001.

Erisman, J. W., Domburg, N., de Vries, W., Kros, H., de Haan, B., and Sanders, K.: The Dutch N-cascade in the European perspective, Science in China Series C: Life Sciences, 48, 827-842, https://doi.org/10.1007/BF03187122, 2005.

Fang, Y., Ye, C., Wang, J., Wu, Y., Hu, M., Lin, W., Xu, F., and Zhu, T.: Relative humidity and O3 concentration as two prerequisites for sulfate formation, Atmos. Chem. Phys., 19, 12295-12307, 10.5194/acp-19-12295-2019, 2019.

Fowler, D., Sutton, M. A., Flechard, C., Cape, J. N., Storeton-West, R., Coyle, M., and Smith, R. I.: The Control of SO2 Dry Deposition on to Natural Surfaces by NH3 and its Effects on Regional Deposition, Water, Air and Soil Pollution: Focus, 1, 39-48, 10.1023/A:1013161912231, 2001.

Fowler, D., Pilegaard, K., Sutton, M. A., Ambus, P., Raivonen, M., Duyzer, J., Simpson, D., Fagerli, H., Fuzzi, S., Schjoerring, J. K., Granier, C., Neftel, A., Isaksen, I. S. A., Laj, P., Maione, M., Monks, P. S., Burkhardt, J., Daemmgen, U., Neirynck, J., Personne, E., Wichink-Kruit, R., Butterbach-Bahl, K., Flechard, C., Tuovinen, J. P., Coyle, M., Gerosa, G., Loubet, B., Altimir, N., Gruenhage, L., Ammann, C., Cieslik, S., Paoletti, E., Mikkelsen, T. N., Ro-Poulsen, H., Cellier, P., Cape, J. N., Horváth, L., Loreto, F., Niinemets, Ü., Palmer, P. I., Rinne, J., Misztal, P., Nemitz, E., Nilsson, D., Pryor, S., Gallagher, M. W., Vesala, T., Skiba, U., Brüggemann, N., Zechmeister-Boltenstern, S., Williams, J., O'Dowd, C., Facchini, M. C., de Leeuw, G., Flossman, A., Chaumerliac, N., and Erisman, J. W.: Atmospheric composition change: Ecosystems–Atmosphere interactions, Atmospheric Environment, 43, 5193-5267, https://doi.org/10.1016/j.atmosenv.2009.07.068, 2009.

Fowler, D., Steadman, C. E., Stevenson, D., Coyle, M., Rees, R. M., Skiba, U. M., Sutton, M. A., Cape, J. N., Dore, A. J., Vieno, M., Simpson, D., Zaehle, S., Stocker, B. D., Rinaldi, M., Facchini, M. C., Flechard, C. R., Nemitz, E., Twigg, M., Erisman, J. W., Butterbach-Bahl, K., and Galloway, J. N.: Effects of global change during the 21st century on the nitrogen cycle, Atmospheric Chemistry and Physics, 15, 13849-13893, 10.5194/acp-15-13849-2015, 2015.

Fowler, D., Brimblecombe, P., Burrows, J., Heal, M. R., Grennfelt, P., Stevenson, D. S., Jowett, A., Nemitz, E., Coyle, M., Liu, X., Chang, Y., Fuller, G. W., Sutton, M. A., Klimont, Z., Unsworth, M. H., and Vieno, M.: A chronology of global air quality, Philosophical Transactions of the Royal Society A: Mathematical, Physical and Engineering Sciences, 378, 20190314, 10.1098/rsta.2019.0314, 2020.

Fu, X., Wang, T., Gao, J., Wang, P., Liu, Y., Wang, S., Zhao, B., and Xue, L.: Persistent Heavy Winter Nitrate Pollution Driven by Increased Photochemical Oxidants in Northern China, Environmental Science & Technology, 54, 3881-3889, 10.1021/acs.est.9b07248, 2020.

Ge, W., Liu, J., Yi, K., Xu, J., Zhang, Y., Hu, X., Ma, J., Wang, X., Wan, Y., Hu, J., Zhang, Z., Wang, X., and Tao, S.: Influence of atmospheric in-cloud aqueous-phase chemistry on the global simulation of SO2 in CESM2, Atmos. Chem. Phys., 21, 16093-16120, 10.5194/acp-21-16093-2021, 2021a.

Ge, Y., Heal, M. R., Stevenson, D. S., Wind, P., and Vieno, M.: Evaluation of global EMEP MSC-W (rv4.34) WRF (v3.9.1.1) model surface concentrations and wet deposition of reactive N and S with measurements, Geosci. Model Dev., 14, 7021-7046, 10.5194/gmd-14-7021-2021, 2021b.

Ge, Y.: Dataset for global sensitivities of reactive N and S gas and particle concentrations and deposition to precursor emissions reductions [Data set], Zenodo, 10.5281/zenodo.7082661, 2022.

Ge, Y., Vieno, M., Stevenson, D. S., Wind, P., and Heal, M. R.: A new assessment of global and regional budgets, fluxes, and lifetimes of atmospheric reactive N and S gases and aerosols, Atmos. Chem. Phys., 22, 8343-8368, 10.5194/acp-22-8343-2022, 2022.

Gu, B., Zhang, L., Van Dingenen, R., Vieno, M., Van Grinsven, H. J. M., Zhang, X., Zhang, S., Chen, Y., Wang, S., Ren, C., Rao, S., Holland, M., Winiwarter, W., Chen, D., Xu, J., and Sutton, M. A.: Abating ammonia is more cost-effective than nitrogen oxides for mitigating PM2.5 air pollution, Science, 374, 758-762, 10.1126/science.abf8623, 2021.

Hart, J. E., Liao, X., Hong, B., Puett, R. C., Yanosky, J. D., Suh, H., Kioumourtzoglou, M.-A., Spiegelman, D., and Laden, F.: The association of long-term exposure to PM2.5 on all-cause mortality in the Nurses' Health Study and the impact of measurement-error correction, Environmental Health, 14, 38, 10.1186/s12940-015-0027-6, 2015.

Hattori, S., Iizuka, Y., Alexander, B., Ishino, S., Fujita, K., Zhai, S., Sherwen, T., Oshima, N., Uemura, R., Yamada, A., Suzuki, N., Matoba, S., Tsuruta, A., Savarino, J., and Yoshida, N.: Isotopic evidence for acidity-driven enhancement of sulfate formation after SO2 emission control, Science Advances, 7, eabd4610, 10.1126/sciadv.abd4610, 2021.

Hauglustaine, D. A., Balkanski, Y., and Schulz, M.: A global model simulation of present and future nitrate aerosols and their direct radiative forcing of climate, Atmospheric Chemistry and Physics, 14, 11031-11063, 10.5194/acp-14-11031-2014, 2014.

Heald, C. L., Collett Jr, J. L., Lee, T., Benedict, K. B., Schwandner, F. M., Li, Y., Clarisse, L., Hurtmans, D. R., Van Damme, M., Clerbaux, C., Coheur, P. F., Philip, S., Martin, R. V., and Pye, H. O. T.: Atmospheric ammonia and particulate inorganic nitrogen over the United States, Atmos. Chem. Phys., 12, 10295-10312, 10.5194/acp-12-10295-2012, 2012.

Hoesly, R. M., Smith, S. J., Feng, L., Klimont, Z., Janssens-Maenhout, G., Pitkanen, T., Seibert, J. J., Vu, L., Andres, R. J., Bolt, R. M., Bond, T. C., Dawidowski, L., Kholod, N., Kurokawa, J. I., Li, M., Liu, L., Lu, Z., Moura, M. C. P., O'Rourke, P. R., and Zhang, Q.: Historical (1750–2014) anthropogenic emissions of reactive gases and aerosols from the Community Emissions Data System (CEDS), Geosci. Model Dev., 11, 369-408, 10.5194/gmd-11-369-2018, 2018.

Hoffmann, E. H., Tilgner, A., Schrödner, R., Bräuer, P., Wolke, R., and Herrmann, H.: An advanced modeling study on the impacts and atmospheric implications of multiphase dimethyl sulfide chemistry, Proceedings of the National Academy of Sciences, 113, 11776, 10.1073/pnas.1606320113, 2016.

Hoffmann, M. R.: On the kinetics and mechanism of oxidation of aquated sulfur dioxide by ozone, Atmospheric Environment (1967), 20, 1145-1154, https://doi.org/10.1016/0004-6981(86)90147-2, 1986.

Holt, J., Selin, N. E., and Solomon, S.: Changes in Inorganic Fine Particulate Matter Sensitivities to Precursors Due to Large-Scale US Emissions Reductions, Environmental Science & Technology, 49, 4834-4841, 10.1021/acs.est.5b00008, 2015.

Iturbide, M., Gutiérrez, J. M., Alves, L. M., Bedia, J., Cerezo-Mota, R., Cimadevilla, E., Cofiño, A. S., Di Luca, A., Faria, S. H., Gorodetskaya, I. V., Hauser, M., Herrera, S., Hennessy, K., Hewitt, H. T., Jones, R. G., Krakovska, S., Manzanas, R., Martínez-Castro, D., Narisma, G. T., Nurhati, I. S., Pinto, I., Seneviratne, S. I., van den Hurk, B., and Vera, C. S.: An update of IPCC climate reference regions for subcontinental analysis of climate model data: definition and aggregated datasets, Earth Syst. Sci. Data, 12, 2959-2970, 10.5194/essd-12-2959-2020, 2020.

Jiang, J., Aksoyoglu, S., Ciarelli, G., Baltensperger, U., and Prévôt, A. S. H.: Changes in ozone and PM2.5 in Europe during the period of 1990–2030: Role of reductions in land and ship emissions, Science of The Total Environment, 741, 140467, https://doi.org/10.1016/j.scitotenv.2020.140467, 2020.

Johnson, M. T., Liss, P. S., Bell, T. G., Lesworth, T. J., Baker, A. R., Hind, A. J., Jickells, T. D., Biswas, K. F., Woodward, E. M. S., and Gibb, S. W.: Field observations of the ocean-atmosphere exchange of ammonia: Fundamental importance of temperature as revealed by a comparison of high and low latitudes, Global Biogeochemical Cycles, 22, https://doi.org/10.1029/2007GB003039, 2008.

Jonson, J. E., Borken-Kleefeld, J., Simpson, D., Nyíri, A., Posch, M., and Heyes, C.: Impact of excess NOx emissions from diesel cars on air quality, public health and eutrophication in Europe, Environmental Research Letters, 12, 094017, 10.1088/1748-9326/aa8850, 2017.

Jonson, J. E., Fagerli, H., Scheuschner, T., and Tsyro, S.: Modelling changes in secondary inorganic aerosol formation and nitrogen deposition in Europe from 2005 to 2030, Atmos. Chem. Phys., 22, 1311-1331, 10.5194/acp-22-1311-2022, 2022.

Jovan, S., Riddell, J., Padgett, P. E., and Nash Iii, T. H.: Eutrophic lichens respond to multiple forms of N: implications for critical levels and critical loads research, Ecological Applications, 22, 1910-1922, https://doi.org/10.1890/11-2075.1, 2012.

Karimi, A., Shirmardi, M., Hadei, M., Birgani, Y. T., Neisi, A., Takdastan, A., and Goudarzi, G.: Concentrations and health effects of short- and long-term exposure to PM2.5, NO2, and O3 in ambient air of Ahvaz city, Iran (2014–2017), Ecotoxicology and Environmental Safety, 180, 542-548, https://doi.org/10.1016/j.ecoenv.2019.05.026, 2019.

Karl, M., Jonson, J. E., Uppstu, A., Aulinger, A., Prank, M., Sofiev, M., Jalkanen, J. P., Johansson, L., Quante, M., and Matthias, V.: Effects of ship emissions on air quality in the Baltic Sea region simulated with three different chemistry transport models, Atmos. Chem. Phys., 19, 7019-7053, 10.5194/acp-19-7019-2019, 2019.

Kelly, J. T., Jang, C., Zhu, Y., Long, S., Xing, J., Wang, S., Murphy, B. N., and Pye, H. O. T.: Predicting the Nonlinear Response of PM2.5 and Ozone to Precursor Emission Changes with a Response Surface Model, Atmosphere, 12, 10.3390/atmos12081044, 2021.

Kharol, S. K., Shephard, M. W., McLinden, C. A., Zhang, L., Sioris, C. E., O'Brien, J. M., Vet, R., Cady-Pereira, K. E., Hare, E., Siemons, J., and Krotkov, N. A.: Dry Deposition of Reactive Nitrogen From Satellite Observations of Ammonia and Nitrogen Dioxide Over North America, Geophysical Research Letters, 45, 1157-1166, https://doi.org/10.1002/2017GL075832, 2018.

Kurokawa, J., and Ohara, T.: Long-term historical trends in air pollutant emissions in Asia: Regional Emission inventory in ASia (REAS) version 3, Atmos. Chem. Phys., 20, 12761-12793, 10.5194/acp-20-12761-2020, 2020.

Le, T., Wang, Y., Liu, L., Yang, J., Yung, Y. L., Li, G., and Seinfeld, J. H.: Unexpected air pollution with marked emission reductions during the COVID-19 outbreak in China, Science, 369, 702-706, 10.1126/science.abb7431, 2020.

Leung, D. M., Shi, H., Zhao, B., Wang, J., Ding, E. M., Gu, Y., Zheng, H., Chen, G., Liou, K.-N., Wang, S., Fast, J. D., Zheng, G., Jiang, J., Li, X., and Jiang, J. H.: Wintertime Particulate Matter Decrease Buffered by Unfavorable Chemical Processes Despite Emissions Reductions in China, Geophysical Research Letters, 47, e2020GL087721, https://doi.org/10.1029/2020GL087721, 2020.

Li, L., Chen, Z. M., Zhang, Y. H., Zhu, T., Li, J. L., and Ding, J.: Kinetics and mechanism of heterogeneous oxidation of sulfur dioxide by ozone on surface of calcium carbonate, Atmos. Chem. Phys., 6, 2453-2464, 10.5194/acp-6-2453-2006, 2006.

Liang, J., and Jacobson, M. Z.: A study of sulfur dioxide oxidation pathways over a range of liquid water contents, pH values, and temperatures, Journal of Geophysical Research: Atmospheres, 104, 13749-13769, https://doi.org/10.1029/1999JD900097, 1999.

Liao, K.-J., Tagaris, E., Napelenok, S. L., Manomaiphiboon, K., Woo, J.-H., Amar, P., He, S., and Russell, A. G.: Current and Future Linked Responses of Ozone and PM2.5 to Emission Controls, Environmental Science & Technology, 42, 4670-4675, 10.1021/es7028685, 2008.

Liu, F., Zhang, Q., van der A, R. J., Zheng, B., Tong, D., Yan, L., Zheng, Y., and He, K.: Recent reduction in NOx emissions over China: synthesis of satellite observations and emission inventories, Environmental Research Letters, 11, 114002, 10.1088/1748-9326/11/11/114002, 2016.

Liu, M., Huang, X., Song, Y., Xu, T., Wang, S., Wu, Z., Hu, M., Zhang, L., Zhang, Q., Pan, Y., Liu, X., and Zhu, T.: Rapid SO2 emission reductions significantly increase tropospheric ammonia concentrations over the North China Plain, Atmos. Chem. Phys., 18, 17933-17943, 10.5194/acp-18-17933-2018, 2018.

Lu, Z., Streets, D. G., Zhang, Q., Wang, S., Carmichael, G. R., Cheng, Y. F., Wei, C., Chin, M., Diehl, T., and Tan, Q.: Sulfur dioxide emissions in China and sulfur trends in East Asia since 2000, Atmos. Chem. Phys., 10, 6311-6331, 10.5194/acp-10-6311-2010, 2010.

Ma, Z., Hu, X., Huang, L., Bi, J., and Liu, Y.: Estimating Ground-Level PM2.5 in China Using Satellite Remote Sensing, Environmental Science & Technology, 48, 7436-7444, 10.1021/es5009399, 2014.

Maahs, H. G.: Kinetics and mechanism of the oxidation of S(IV) by ozone in aqueous solution with particular reference to SO2 conversion in nonurban tropospheric clouds, Journal of Geophysical Research: Oceans, 88, 10721-10732, https://doi.org/10.1029/JC088iC15p10721, 1983.

Massad, R. S., Nemitz, E., and Sutton, M. A.: Review and parameterisation of bi-directional ammonia exchange between vegetation and the atmosphere, Atmos. Chem. Phys., 10, 10359-10386, 10.5194/acp-10-10359-2010, 2010.

McArdle, J. V., and Hoffmann, M. R.: Kinetics and mechanism of the oxidation of aquated sulfur dioxide by hydrogen peroxide at low pH, The Journal of Physical Chemistry, 87, 5425-5429, 10.1021/j150644a024, 1983.

McDuffie, E. E., Fibiger, D. L., Dubé, W. P., Lopez-Hilfiker, F., Lee, B. H., Thornton, J. A., Shah, V., Jaeglé, L., Guo, H., Weber, R. J., Michael Reeves, J., Weinheimer, A. J., Schroder, J. C., Campuzano-Jost, P., Jimenez, J. L., Dibb, J. E., Veres, P., Ebben, C., Sparks, T. L., Wooldridge, P. J., Cohen, R. C., Hornbrook, R. S., Apel, E. C., Campos, T., Hall, S. R., Ullmann, K., and Brown, S. S.: Heterogeneous N2O5 Uptake During Winter: Aircraft Measurements During the 2015 WINTER Campaign and Critical Evaluation of Current Parameterizations, Journal of Geophysical Research: Atmospheres, 123, 4345-4372, https://doi.org/10.1002/2018JD028336, 2018.

McFiggans, G., Mentel, T. F., Wildt, J., Pullinen, I., Kang, S., Kleist, E., Schmitt, S., Springer, M., Tillmann, R., Wu, C., Zhao, D., Hallquist, M., Faxon, C., Le Breton, M., Hallquist, Å. M., Simpson, D., Bergström, R., Jenkin, M. E., Ehn, M., Thornton, J. A., Alfarra, M. R., Bannan, T. J., Percival, C. J., Priestley, M., Topping, D., and Kiendler-Scharr, A.: Secondary organic aerosol reduced by mixture of atmospheric vapours, Nature, 565, 587-593, 10.1038/s41586-018-0871-y, 2019.

McHale, M. R., Ludtke, A. S., Wetherbee, G. A., Burns, D. A., Nilles, M. A., and Finkelstein, J. S.: Trends in precipitation chemistry across the U.S. 1985–2017: Quantifying the benefits from 30 years of Clean Air Act amendment regulation, Atmospheric Environment, 247, 118219, https://doi.org/10.1016/j.atmosenv.2021.118219, 2021.

Megaritis, A. G., Fountoukis, C., Charalampidis, P. E., Pilinis, C., and Pandis, S. N.: Response of fine particulate matter concentrations to changes of emissions and temperature in Europe, Atmos. Chem. Phys., 13, 3423-3443, 10.5194/acp-13-3423-2013, 2013.

Meng, F., Zhang, Y., Kang, J., Heal, M. R., Reis, S., Wang, M., Liu, L., Wang, K., Yu, S., Li, P., Wei, J., Hou, Y., Zhang, Y., Liu, X., Cui, Z., Xu, W., and Zhang, F.: Trends in secondary inorganic aerosol pollution in China and its responses to emission controls of precursors in wintertime, Atmos. Chem. Phys., 22, 6291-6308, 10.5194/acp-22-6291-2022, 2022.

Metzger, S., Steil, B., Abdelkader, M., Klingmüller, K., Xu, L., Penner, J. E., Fountoukis, C., Nenes, A., and Lelieveld, J.: Aerosol water parameterisation: a single parameter framework, Atmos. Chem. Phys., 16, 7213-7237, 10.5194/acp-16-7213-2016, 2016.

Metzger, S., Abdelkader, M., Steil, B., and Klingmüller, K.: Aerosol water parameterization: long-term evaluation and importance for climate studies, Atmos. Chem. Phys., 18, 16747-16774, 10.5194/acp-18-16747-2018, 2018.

NEC: National Emission Ceilings (NEC) Directive reporting status, Briefing no. 2/2019, PDF TH-AM-19-003-EN-N, available at: https://www.eea.europa.eu/themes/air/air-pollution-sources-1/national-emission-ceilings/nec-directive-reporting-status-2019 (last access: 07 August 2022), 2019.

Nemitz, E., Sutton, M. A., Wyers, G. P., and Jongejan, P. A. C.: Gas-particle interactions above a Dutch heathland: I. Surface exchange fluxes of NH3, SO2, HNO3 and HCl, Atmospheric Chemistry and Physics, 4, 989-1005, 10.5194/acp-4-989-2004, 2004.

Nenes, A., Pandis, S. N., Weber, R. J., and Russell, A.: Aerosol pH and liquid water content determine when particulate matter is sensitive to ammonia and nitrate availability, Atmos. Chem. Phys., 20, 3249-3258, 10.5194/acp-20-3249-2020, 2020.

Novak, G. A., Kilgour, D. B., Jernigan, C. M., Vermeuel, M. P., and Bertram, T. H.: Oceanic emissions of dimethyl sulfide and methanethiol and their contribution to sulfur dioxide production in the marine atmosphere, Atmos. Chem. Phys., 22, 6309-6325, 10.5194/acp-22-6309-2022, 2022.

Penkett, S. A., Jones, B. M. R., Brich, K. A., and Eggleton, A. E. J.: The importance of atmospheric ozone and hydrogen peroxide in oxidising sulphur dioxide in cloud and rainwater, Atmospheric Environment (1967), 13, 123-137, https://doi.org/10.1016/0004-6981(79)90251-8, 1979.

Pescott, O. L., Simkin, J. M., August, T. A., Randle, Z., Dore, A. J., and Botham, M. S.: Air pollution and its effects on lichens, bryophytes, and lichen-feeding Lepidoptera: review and evidence from biological records, Biological Journal of the Linnean Society, 115, 611-635, 10.1111/bij.12541, 2015.

Pommier, M., Fagerli, H., Gauss, M., Simpson, D., Sharma, S., Sinha, V., Ghude, S. D., Landgren, O., Nyiri, A., and Wind, P.: Impact of regional climate change and future emission scenarios on surface O3 and PM2.5 over India, Atmos. Chem. Phys., 18, 103-127, 10.5194/acp-18-103-2018, 2018.

Pommier, M., Fagerli, H., Schulz, M., Valdebenito, A., Kranenburg, R., and Schaap, M.: Prediction of source contributions to urban background PM10 concentrations in European cities: a case study for an episode in December 2016 using EMEP/MSC-W rv4.15 and LOTOS-EUROS v2.0 – Part 1: The country contributions, Geoscientific Model Development, 13, 1787-1807, 10.5194/gmd-13-1787-2020, 2020.

Pozzer, A., Tsimpidi, A. P., Karydis, V. A., de Meij, A., and Lelieveld, J.: Impact of agricultural emission reductions on fine-particulate matter and public health, Atmos. Chem. Phys., 17, 12813-12826, 10.5194/acp-17-12813-2017, 2017.
Quinn, P. K., and Bates, T. S.: The case against climate regulation via oceanic phytoplankton sulphur emissions, Nature, 480, 51-56, 10.1038/nature10580, 2011.
Riemer, N., Vogel, H., Vogel, B., Schell, B., Ackermann, I., Kessler, C., and Hass, H.: Impact of the heterogeneous hydrolysis of N2O5 on chemistry and nitrate aerosol formation in the lower troposphere under photosmog conditions, Journal of Geophysical Research: Atmospheres, 108, 4144, 10.1029/2002JD002436, 2003.
Riddick, S. N., Dragosits, U., Blackall, T. D., Tomlinson, S. J., Daunt, F., Wanless, S., Hallsworth, S., Braban, C. F., Tang, Y. S., and Sutton, M. A.: Global assessment of the effect of climate change on ammonia emissions from seabirds, Atmospheric Environment, 184, 212-223, https://doi.org/10.1016/j.atmosenv.2018.04.038, 2018.
Sadavarte, P., and Venkataraman, C.: Trends in multi-pollutant emissions from a technology-linked inventory for India: I. Industry and transport sectors, Atmospheric Environment, 99, 353-364, https://doi.org/10.1016/j.atmosenv.2014.09.081, 2014.
Saylor, R., Myles, L., Sibble, D., Caldwell, J., and Xing, J.: Recent trends in gas-phase ammonia and PM2.5 ammonium in the Southeast United States, Journal of the Air & Waste Management Association, 65, 347-357, 10.1080/10962247.2014.992554, 2015.
Seinfeld, J. H., and Pandis, S. N.: Atmospheric chemistry and physics: from air pollution to climate change, John Wiley & Sons, 2016.
Sheng, F., Jingjing, L., Yu, C., Fu-Ming, T., Xuemei, D., and Jing-yao, L.: Theoretical study of the oxidation reactions of sulfurous acid/sulfite with ozone to produce sulfuric acid/sulfate with atmospheric implications, RSC Advances, 8, 7988-7996, 10.1039/C8RA00411K, 2018.
Sheppard, L. J., Leith, I. D., Mizunuma, T., Neil Cape, J., Crossley, A., Leeson, S., Sutton, M. A., van Dijk, N., and Fowler, D.: Dry deposition of ammonia gas drives species change faster than wet deposition of ammonium ions: evidence from a long-term field manipulation, Global Change Biology, 17, 3589-3607, https://doi.org/10.1111/j.1365-2486.2011.02478.x, 2011.
Simpson, D., Benedictow, A., Berge, H., Bergström, R., Emberson, L. D., Fagerli, H., Flechard, C. R., Hayman, G. D., Gauss, M., Jonson, J. E., Jenkin, M. E., Nyíri, A., Richter, C., Semeena, V. S., Tsyro, S., Tuovinen, J. P., Valdebenito, Á., and Wind, P.: The EMEP MSC-W chemical transport model — technical description, Atmos. Chem. Phys., 12, 7825-7865, 10.5194/acp-12-7825-2012, 2012.
Simpson, D., Schulz, M., Semeena, V. S., Tsyro, S., Valdebenito, A., Wind, P., and Steensen, B. M.: EMEP model development and performance changes, in EMEP Status Report 1/2013, Norwegian Meteorological Institute, Oslo, Norway, www.emep.int, 45-57, https://emep.int/publ/reports/2013/EMEP_status_report_1_2013.pdf, 2013.
Simpson, D., Tsyro, S., and Wind, P.: Updates to the EMEP/MSC-W model, in EMEP Status Report 1/2015, Norwegian Meteorological Institute, Oslo, Norway, www.emep.int, 129-136, https://emep.int/publ/reports/2015/EMEP_Status_Report_1_2015.pdf, 2015.
Simpson, D., Nyíri, A. g., Tsyro, S., Valdebenito, Á., and Wind, P.: Updates to the EMEP/MSC-W model, 2015-2016, in EMEP Status Report 1/2016, Norwegian Meteorological Institute, Oslo, Norway, www.emep.int, 131-138, https://emep.int/publ/reports/2016/EMEP_Status_Report_1_2016.pdf, 2016.
Simpson, D., Bergström, R., Imhof, H., and Wind, P.: Updates to the EMEP/MSC-W model 2016--2017, in EMEP Status Report 1/2017, Norwegian Meteorological Institute, Oslo, Norway, www.emep.int, 115-122, https://emep.int/publ/reports/2017/EMEP_Status_Report_1_2017.pdf, 2017.
Simpson, D., Wind, P., Bergström, R., Gauss, M., Tsyro, S., and Valdebenito, Á.: Updates to the EMEP MSC-W model 2017-2018, in EMEP Status Report 1/2018, Norwegian Meteorological Institute, Oslo, Norway, www.emep.int, 107-115, https://emep.int/publ/reports/2018/EMEP_Status_Report_1_2018.pdf, 2018.
Simpson, D., Bergström, R., Tsyro, S., and Wind, P.: Updates to the EMEP/MSC-W model 2018–2019, in EMEP Status Report 1/2019, Norwegian Meteorological Institute, Oslo, Norway, www.emep.int, 143-152, https://emep.int/publ/reports/2019/EMEP_Status_Report_1_2019.pdf, 2019.
Simpson, D., Bergström, R., Tsyro, S., and Wind, P.: Updates to the EMEP MSC-W model 2019–2020, in EMEP Status Report 1/2020, Norwegian Meteorological Institute, Oslo, Norway, www.emep.int, 153-163, https://emep.int/publ/reports/2020/EMEP_Status_Report_1_2020.pdf, 2020.
Skamarock, W. C., Klemp, J. B., Dudhia, J., Gill, D. O., Barker, D., Duda, M. G., Huang, X. Y., Wang, W., and Powers, J. G.: A Description of the Advanced Research WRF Version 3 (No. NCAR/TN-475+STR), University Corporation for Atmospheric Research, 113, 10.5065/D68S4MVH, 2008.
Smith, R. I., Fowler, D., Sutton, M. A., Flechard, C., and Coyle, M.: Regional estimation of pollutant gas dry deposition in the UK: model description, sensitivity analyses and outputs, Atmospheric Environment, 34, 3757-3777, https://doi.org/10.1016/S1352-2310(99)00517-8, 2000.
Stieb, D. M., Evans, G. J., To, T. M., Brook, J. R., and Burnett, R. T.: An ecological analysis of long-term exposure to PM2.5 and incidence of COVID-19 in Canadian health regions, Environmental Research, 191, 110052, https://doi.org/10.1016/j.envres.2020.110052, 2020.
Sun, J., Fu, J. S., Lynch, J. A., Huang, K., and Gao, Y.: Climate-driven exceedance of total (wet + dry) nitrogen (N) + sulfur (S) deposition to forest soil over the conterminous U.S, Earth's Future, 5, 560-576, https://doi.org/10.1002/2017EF000588, 2017.
Sutton, M. A., Asman, W. A. H., and Schøring, J. K.: Dry deposition of reduced nitrogen, Tellus B: Chemical and Physical Meteorology, 46, 255-273, 10.3402/tellusb.v46i4.15796, 1994.
Sutton, M. A., Reis, S., Riddick, S. N., Dragosits, U., Nemitz, E., Theobald, M. R., Tang, Y. S., Braban, C. F., Vieno, M., Dore, A. J., Mitchell, R. F., Wanless, S., Daunt, F., Fowler, D., Blackall, T. D., Milford, C., Flechard, C. R., Loubet, B.,

Massad, R., Cellier, P., Personne, E., Coheur, P. F., Clarisse, L., Van Damme, M., Ngadi, Y., Clerbaux, C., Skjøth, C. A., Geels, C., Hertel, O., Wichink Kruit, R. J., Pinder, R. W., Bash, J. O., Walker, J. T., Simpson, D., Horváth, L., Misselbrook, T. H., Bleeker, A., Dentener, F., and de Vries, W.: Towards a climate-dependent paradigm of ammonia emission and deposition, Philosophical Transactions of the Royal Society B: Biological Sciences, 368, 20130166, 10.1098/rstb.2013.0166, 2013.

Sutton, M. A., Mason, K. E., Sheppard, L. J., Sverdrup, H., Haeuber, R., and Hicks, W. K.: Nitrogen Deposition, Critical Loads and Biodiversity, Springer, Dordrecht, 535 pp., 2014.

Sutton, M. A., van Dijk, N., Levy, P. E., Jones, M. R., Leith, I. D., Sheppard, L. J., Leeson, S., Sim Tang, Y., Stephens, A., Braban, C. F., Dragosits, U., Howard, C. M., Vieno, M., Fowler, D., Corbett, P., Naikoo, M. I., Munzi, S., Ellis, C. J., Chatterjee, S., Steadman, C. E., Móring, A., and Wolseley, P. A.: Alkaline air: changing perspectives on nitrogen and air pollution in an ammonia-rich world, Philosophical Transactions of the Royal Society A: Mathematical, Physical and Engineering Sciences, 378, 20190315, 10.1098/rsta.2019.0315, 2020.

Szopa, S., Naik V., Adhikary B., Artaxo P., Berntsen T., Collins W.D., Fuzzi S., Gallardo L., Kiendler-Scharr A., Klimont Z., Liao H., Unger N., and P., Z.: Short-Lived Climate Forcers. In Climate Change 2021: The Physical Science Basis. Contribution of Working Group I to the Sixth Assessment Report of the Intergovernmental Panel on Climate Change, Cambridge University Press, Cambridge, United Kingdom and New York, NY, USA, 817-922, 10.1017/9781009157896.008, 2021.

Theobald, M. R., Vivanco, M. G., Aas, W., Andersson, C., Ciarelli, G., Couvidat, F., Cuvelier, K., Manders, A., Mircea, M., Pay, M. T., Tsyro, S., Adani, M., Bergström, R., Bessagnet, B., Briganti, G., Cappelletti, A., D'Isidoro, M., Fagerli, H., Mar, K., Otero, N., Raffort, V., Roustan, Y., Schaap, M., Wind, P., and Colette, A.: An evaluation of European nitrogen and sulfur wet deposition and their trends estimated by six chemistry transport models for the period 1990–2010, Atmos. Chem. Phys., 19, 379-405, 10.5194/acp-19-379-2019, 2019.

Thunis, P., Clappier, A., Pisoni, E., and Degraeuwe, B.: Quantification of non-linearities as a function of time averaging in regional air quality modeling applications, Atmospheric Environment, 103, 263-275, https://doi.org/10.1016/j.atmosenv.2014.12.057, 2015.

Thunis, P., Clappier, A., Beekmann, M., Putaud, J. P., Cuvelier, C., Madrazo, J., and de Meij, A.: Non-linear response of PM2.5 to changes in NOx and NH3 emissions in the Po basin (Italy): consequences for air quality plans, Atmos. Chem. Phys., 21, 9309-9327, 10.5194/acp-21-9309-2021, 2021.

Tørseth, K., Aas, W., Breivik, K., Fjæraa, A. M., Fiebig, M., Hjellbrekke, A. G., Lund Myhre, C., Solberg, S., and Yttri, K. E.: Introduction to the European Monitoring and Evaluation Programme (EMEP) and observed atmospheric composition change during 1972-2009, Atmos. Chem. Phys., 12, 5447-5481, 10.5194/acp-12-5447-2012, 2012.

Tsimpidi, A. P., Karydis, V. A., and Pandis, S. N.: Response of Inorganic Fine Particulate Matter to Emission Changes of Sulfur Dioxide and Ammonia: The Eastern United States as a Case Study, Journal of the Air & Waste Management Association, 57, 1489-1498, 10.3155/1047-3289.57.12.1489, 2007.

Tsimpidi, A. P., Karydis, V. A., and Pandis, S. N.: Response of Fine Particulate Matter to Emission Changes of Oxides of Nitrogen and Anthropogenic Volatile Organic Compounds in the Eastern United States, Journal of the Air & Waste Management Association, 58, 1463-1473, 10.3155/1047-3289.58.11.1463, 2008.

Tsyro, S., Karl, M., Simpson, D., Valdebenito, A. l., and Wind, P.: Updates to the EMEP/MSC-W model, in EMEP Status Report 1/2014, Norwegian Meteorological Institute, Oslo, Norway, www.emep.int, 143-146, https://emep.int/publ/reports/2014/EMEP_Status_Report_1_2014.pdf, 2014.

USEPA: Report on the Environment: Particulate Matter Concentrations., United States Environmental Protection Agency, available at : https://cfpub.epa.gov/roe/indicator.cfm?i=9 (last access: 7 August 2022), 2017.

Van Herk, C. M., Mathijssen-Spiekman, E. A. M., and de Zwart, D.: Long distance nitrogen air pollution effects on lichens in Europe, The Lichenologist, 35, 347-359, 10.1016/S0024-2829(03)00036-7, 2003.

Vasilakos, P., Russell, A., Weber, R., and Nenes, A.: Understanding nitrate formation in a world with less sulfate, Atmos. Chem. Phys., 18, 12765-12775, 10.5194/acp-18-12765-2018, 2018.

Vieno, M., Dore, A. J., Stevenson, D. S., Doherty, R., Heal, M. R., Reis, S., Hallsworth, S., Tarrason, L., Wind, P., Fowler, D., Simpson, D., and Sutton, M. A.: Modelling surface ozone during the 2003 heat-wave in the UK, Atmospheric Chemistry and Physics, 10, 7963-7978, 10.5194/acp-10-7963-2010, 2010.

Sutton, M. A., Reis, S., Baker, S. M. H., Wolseley, P. A., Leith, I. D., van Dijk, N., Tang, Y. S., James, P. W., Theobald, M. R., and Whitfield, C.: Estimation of the Ammonia Critical Level for Epiphytic Lichens Based on Observations at Farm, Landscape and National Scales, Atmospheric ammonia, 71-86, 10.1007/978-1-4020-9121-6_6, 2009.

Vieno, M., Heal, M. R., Hallsworth, S., Famulari, D., Doherty, R. M., Dore, A. J., Tang, Y. S., Braban, C. F., Leaver, D., Sutton, M. A., and Reis, S.: The role of long-range transport and domestic emissions in determining atmospheric secondary inorganic particle concentrations across the UK, Atmos. Chem. Phys., 14, 8435-8447, 10.5194/acp-14-8435-2014, 2014.

Vieno, M., Heal, M. R., Williams, M. L., Carnell, E. J., Nemitz, E., Stedman, J. R., and Reis, S.: The sensitivities of emissions reductions for the mitigation of UK PM2.5, Atmospheric Chemistry and Physics, 16, 265-276, 10.5194/acp-16-265-2016, 2016.

Wang, S., Xing, J., Jang, C., Zhu, Y., Fu, J. S., and Hao, J.: Impact Assessment of Ammonia Emissions on Inorganic Aerosols in East China Using Response Surface Modeling Technique, Environmental Science & Technology, 45, 9293-9300, 10.1021/es2022347, 2011.

Wang, Y., Zhang, Q. Q., He, K., Zhang, Q., and Chai, L.: Sulfate-nitrate-ammonium aerosols over China: response to 2000–2015 emission changes of sulfur dioxide, nitrogen oxides, and ammonia, Atmos. Chem. Phys., 13, 2635-2652, 10.5194/acp-13-2635-2013, 2013.

Warner, J. X., Dickerson, R. R., Wei, Z., Strow, L. L., Wang, Y., and Liang, Q.: Increased atmospheric ammonia over the world's major agricultural areas detected from space, Geophysical Research Letters, 44, 2875-2884, https://doi.org/10.1002/2016GL072305, 2017.
Weber, R. J., Guo, H., Russell, A. G., and Nenes, A.: High aerosol acidity despite declining atmospheric sulfate concentrations over the past 15 years, Nature Geoscience, 9, 282-285, 10.1038/ngeo2665, 2016.
Werner, M., Kryza, M., and Wind, P.: High resolution application of the EMEP MSC-W model over Eastern Europe – Analysis of the EMEP4PL results, Atmospheric Research, 212, 6-22, https://doi.org/10.1016/j.atmosres.2018.04.025, 2018.
WHO: World Health Organization global air quality guidelines: particulate matter (PM2.5 and PM10), ozone, nitrogen dioxide, sulfur dioxide and carbon monoxide, World Health Organization, Geneva, 74-78, 2021.
Xu, L., and Penner, J. E.: Global simulations of nitrate and ammonium aerosols and their radiative effects, Atmos. Chem. Phys., 12, 9479-9504, 10.5194/acp-12-9479-2012, 2012.
Yi, W., Shen, J., Liu, G., Wang, J., Yu, L., Li, Y., Reis, S., and Wu, J.: High NH3 deposition in the environs of a commercial fattening pig farm in central south China, Environmental Research Letters, 16, 125007, 10.1088/1748-9326/ac3603, 2021.
Yu, F., Nair, A. A., and Luo, G.: Long-Term Trend of Gaseous Ammonia Over the United States: Modeling and Comparison With Observations, Journal of Geophysical Research: Atmospheres, 123, 8315-8325, https://doi.org/10.1029/2018JD028412, 2018.
Zheng, B., Tong, D., Li, M., Liu, F., Hong, C., Geng, G., Li, H., Li, X., Peng, L., Qi, J., Yan, L., Zhang, Y., Zhao, H., Zheng, Y., He, K., and Zhang, Q.: Trends in China's anthropogenic emissions since 2010 as the consequence of clean air actions, Atmos. Chem. Phys., 18, 14095-14111, 10.5194/acp-18-14095-2018, 2018.